ISSN 0972-5741 Volume 114 October 2017

IGC Newsletter

IN THIS ISSUE

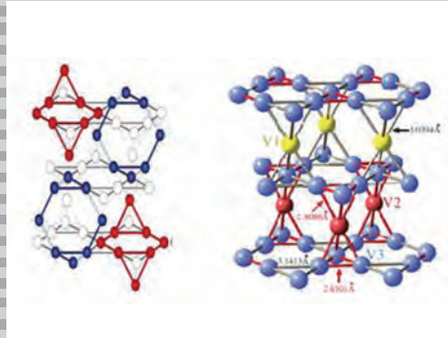

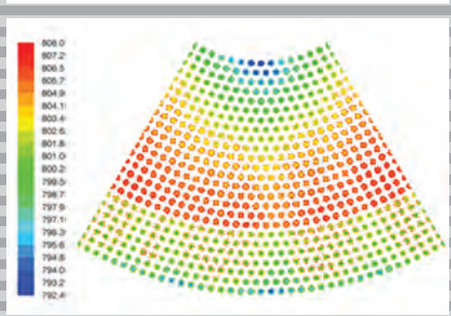

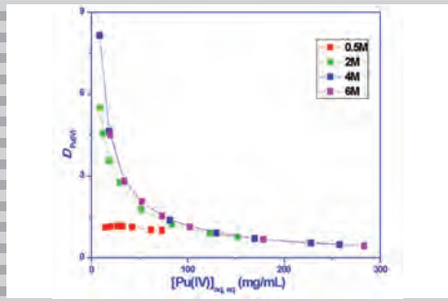

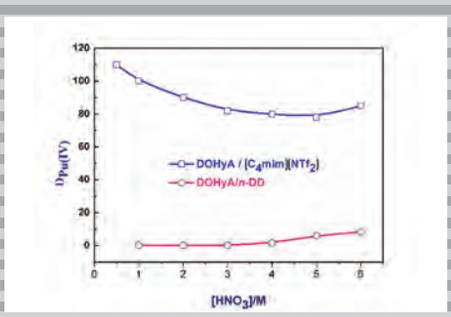

INDIRA GANDHI CENTRE FOR ATOMIC RESEARCH
http://www.igcar.gov.in/lis/nl114/igc114.pdf

From the Editorial Committee

Dear Reader

Greeting from the new Editorial Committee. We look forward with great enthusiasm to carry out the task of showcasing the technical achievements of our Centre every quarter, with the inputs from various Groups.

It is our pleasant privilege to forward a copy of the latest issue of IGC Newsletter (Volume 114, October 2017 issue)

In the first technical article Dr. S. Kalavathi and colleagues have discussed about "The Physics of Charge Frustrated Systems".

In the second technical article Shri P. Puthiyavinayagam and colleagues have described about "High Fidelity Computational Modelling of Intermediate Heat Exchangers and Steam Generators for Future FBR".

This issue's young officer's forum features an article by Dr. Balija Sreenivasulu on "Tri-iso-amyl Phosphate: A Potential Extractant for the Reprocessing of Spent Nuclear Fuels".

Dr. R. Rama has shared her experience in Room Temperature Ionic Liquids (RTILs) for Solvent Extraction and Electrochemical Studies of Lanthanides and Actinides in young researcher's forum.

This Newsletter carries reports on the "International Conference on Electron Microscopy and Allied Techniques (EMSI-2017)", "Bridge Course on Non-destructive Evaluation (BRIC-NDE)", "Summer Training in Physics and Chemistry (STIPAC-2017)", "BITS Practice School", "Graduation Function of the 11th Batch of Trainee Scientific Officers of BARC Training School at IGCAR" and "Quality Circle Annual Meet (QCAM)-2017".

We are happy to share with you the awards, honors and distinctions earned by our colleagues.

We look forward to your comments, continued guidance and support.

Editorial Committee, IGC Newsletter

The Physics of Charge Frustrated Systems

Electron correlation in condensed matter always throws up a plethora of novel, exotic and complex phenomena that routinely destabilize every attempt to formulate or formalize an all encompassing understanding. In the last few decades several challenges have been posed by the high temperature superconductors, colossal magneto resistance materials, spin glasses, frustrated systems and so on. Experimental and theoretical tools have been stretched to their limits to comprehend the complexities, but the horizon of convergence appears to recede farther and farther. Amongst the complex, correlated condensed matter systems, 'frustrated systems' is a class in itself. Such systems may arise due to the frustration of charge or spin.

What is meant by frustration in condensed matter systems? Matter assumes a crystalline form by occupying discrete space locations, constrained by symmetry and inter particle interaction. In general, the spatial organization coupled with the commensurate interaction results in myriad observed properties and ultimately a unique ground state. But then, whenever a conflict arises between some fundamental interaction and the underlying lattice geometry, a geometrical frustration results. The effect of such a geometrical frustration is the appearance of finite entropy at zero Kelvin, indicating existence of a degenerate ground state. With the possibility of existence of degenerate ground state, the ultimate realizations can be of various kinds. The system can continue to be in the fluctuating degenerate state and end up as a novel ground state like spin liquid or it can freeze in one of the disordered states as spin ice or the degeneracy can be lifted and the system can develop a different long range order manifesting as a structural transition. A typical example where frustration emerges is, when an antiferromagnetic alignment of three spins is imposed on a triangular lattice. When two of the spins are aligned anti parallel, it is impossible to place the third spin opposite to both these spins and this situation is called spin frustration. Inherently, a few of the lattices namely, the triangular lattice ($P6_3/mmc$), the Kagome lattice ($P6_3/mmc$) and the pyrochlore lattice (Fd-3m) shown in Figure1 sustain frustration.

Short range order and infinite configurations

The recognition of the existence of such a geometrical frustration dates back to 1936 when Giaque and Stout measured specific heat on hexagonal water-ice (Ih, ($P6_3/mmc$)) and showed finite entropy (0.8 cal/deg/mole) at zero Kelvin which was explained by Linus Pauling by considering the configurational entropy using the Bernal-Fowler ice-rules. Ordering of the oxygen and hydrogen ions in the hexagonal ice demonstrates that whenever pyrochlore lattice is to be occupied by species with a specific pair-wise interaction, a degenerate ground state must be anticipated. The recognition of frustration and finite entropy in water ice has resulted in modeling spins on triangular and pyrochlore lattices. Earliest calculations by Wannier (1950) consider the case of Ising spins on triangular lattice and show that the ground state is macroscopically degenerate. Subsequently Anderson (1956) considered ordering of cations in the pyrochlore B-sub lattice of a spinel system. He showed that if there are two kinds of cations trying to occupy the corner shared tetrahedra (say N number of them) in the pyrochlore sub-lattice, with the constraint that the tetrahedra should be maximally occupied by both the cations, (now known as Anderson's 2:2 criterion) the number of possible configurations can be worked out to be:

$$W = \left(\frac{3}{8}\right)^{\frac{N}{4}} . 6^{\frac{N}{4}}$$

Thus with frustration there is a short range order and almost

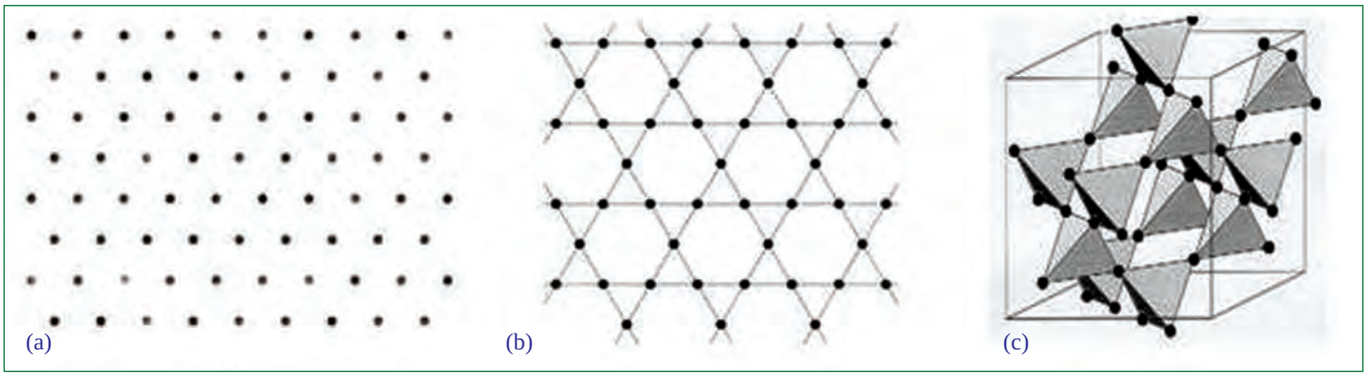

Figure 1: (a) Triangular Lattice, (b) Kagome Lattice and (c) Pyrochlore Lattice

infinite number of possible configurations leading to the loss of the uniqueness of the ground state.

Spinels exhibiting charge ordering from frustration

Spinels are materials with structural formula AB_2O_4 and the structure can be viewed as comprising of A^{2+} and B^{3+} ions. The 'A' ions occupy the tetrahedral voids and the 'B' ions occupy the octahedral voids in a normal spinel. If 'A' ions occupy the tetrahedral voids and 'A' and 'B' ions occupy the octahedral voids it is called an inverse spinel. Charge disproportionation becomes inevitable in the B- sub-lattice of a normal spinel, if A happens to be A^{1+} or A^{3+}. Such a charge disproportionation on the pyrochlore lattice results in "frustration', namely an infinite possibility of configurations. Experimentally such a system was realized for the first time in magnetite (Fe_3O_4). In 1939, Verwey reported an anomalous increase in resistance when inverse spinel Fe_3O_4 was cooled to around 125 K, now known as Verwey Temperature (Tv). Subsequent X-ray analyses prompted him to suggest a model for the inverse spinel Fe_3O_4, where 50% of the Fe^{3+} occupies the tetrahedral voids and the remaining 50% of Fe^{3+} and Fe^{2+} occupy the octahedral voids (namely the B-site). He proposed that the Fe^{2+} and Fe^{3+} ions occupying the B site, forming the pyrochlore sub-lattice are randomly placed (frustrated) on the tetrahedra above T_v and are ordered below that temperature. It was by and large believed that the ordering would be as per Anderson's 2:2 criteria. Though the nature and mechanism of ordering were contested for over four decades, the existence of the transition on a multitude of specimens stood the test of time. Apart from the magnetite Fe_3O_4 only four more spinel compounds have so far shown charge ordering transition from frustration. They are $LiMn_2O_4$, $CuIr_2S_4$, AlV_2O_4 and $LiRh_2O_4$. In all these five compounds charge ordering from frustration is associated with structural transition that is always tied up with change from semiconducting to localized behavior. Table shown here summarizes the transition temperatures and the charge ordered structures in the five spinel oxides known so far that exhibit charge ordering transition from frustration.

It is interesting to see that the structures of the charge ordered state and the transition temperatures are different in each one of them. In all of them the transition metal ion occupying the pyrochlore B-sub-lattice has multiple valences. It is to be noticed that amongst them AlV_2O_4 is unique since it remains in the charge ordered state at ambient temperature. This aspect enables probing further into the charge ordered state at convenient ambient temperature.

Formation of multimer molecular units as a result of charge ordering

While the nature of ordered structure in Fe_3O_4 was still being debated during 1990s, structural transition in the 'battery material' $LiMn_2O_4$ posed further challenge. The structural transition at 290 K that proved to be a hindrance for the battery performance was initially regarded as due to Jahn-Teller distortion of Mn ions. But soon detailed analysis of XRD and electron diffraction showed that $LiMn_2O_4$ undergoes a structural phase transition from a charge frustrated high temperature cubic structure to a charge ordered orthorhombic structure. The most significant factor that characterizes the charge ordered state which is a '3a x 3a x a' superstructure of the high temperature cubic structure is the Mn-O bond distance. While in the cubic (Fd-3m) spinel phase there is a unique Mn-O distance of 1.96 Å, the charge ordered orthorhombic (Fddd) structure with five different Mn sites shows two different Mn-O distances; two of the Mn sites show an Mn-O bond distance of 1.91 Å indicating the existence of Mn^{4+} and the other three of them show an Mn-O bond distance of 2.01 Å that correspond to Mn^{3+} as confirmed by EXAFS measurements.

The charge ordered structure proposed by Rodriguez-Carvajaal brings forth a columnar ordering of Mn^{3+} and Mn^{4+}, in such a way that two kinds of columns of Mn^{3+} one including a Li at the centre and the other without a Li are surrounded by octagonal cylinders of Mn^{4+} as shown in Figure 2a. Notice that the figure shown here is the projection along [001] ; Green-Li; Blue- Mn^{3+}; Magenta-Mn^{4+}; oxygen atoms are removed for clarity. The ordering of charges in this system is unique and different from the charge ordering in perovskites where frustration is not in the picture.

In the case of $CuIr_2O_4$ the charge ordered triclinic structure occurs below 230 K. In this system Cu is in +1 state and hence Ir should assume a valency of 3.5 which is achieved by Ir^{3+} and Ir^{4+}. Detailed analysis of X-ray diffraction, electron diffraction and

Table 1: Spinels exhibiting charge order

Spinel Compound	Charge ordered structure	Charge order temperature (K)	Nature of ordering
Fe_3O_4	Monoclinic (Cc)	126	Formation of trimerons
$LiMn_2O_4$	Orthorhombic (Fddd)	290	Octagonal Columnar units
$CuIr_2S_4$	Triclinic (P-1)	230	Formation of Octamers
AlV_2O_4	Rhombohedral(R-3m)	700	Formation of heptamers
$LiRh_2O_4$	Tetragonal($I4_1/amd$) and Orthorhombic	230 & 170	Nature of ordering unknown

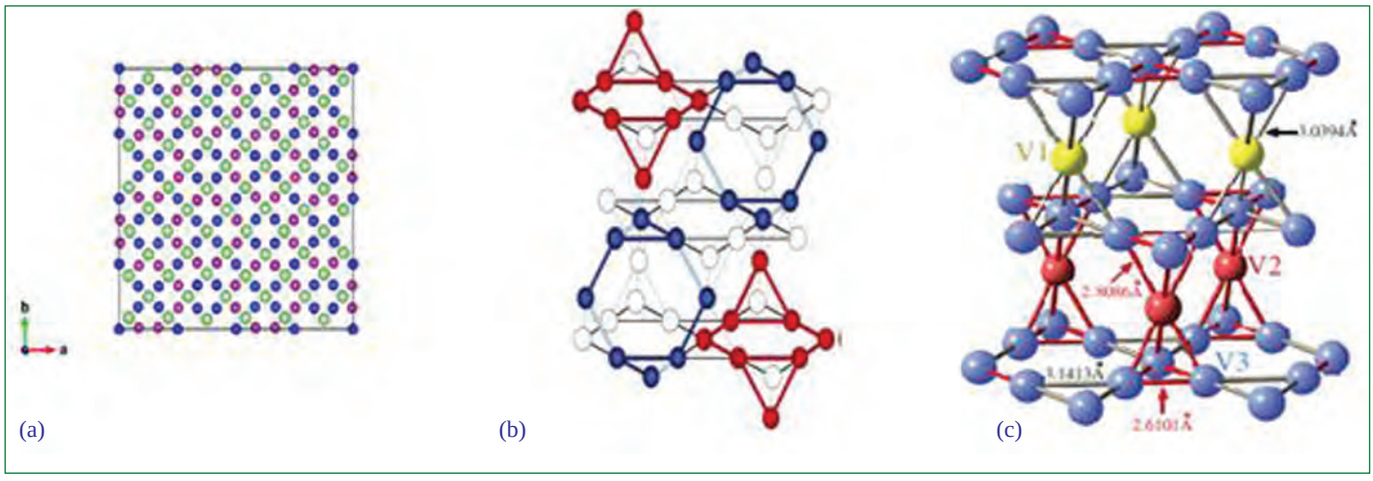

Figure 2: (a) Columnar ordering in $LiMn_2O_4$, (b) formation of Ir octamers in $CuIr_2S_4$ and (c) formation of V heptamers in AlV_2O_4

neutron diffraction data put together threw up yet another complex ordering in this system. The ordered triclinic structure shows eight in-equivalent Ir sites forming octamer molecular units. Figure 2b shows the formation of octamers with Ir^{3+} (red) and Ir^{4+} (blue) in $CuIr_2S_4$ when viewed in the [111] cubic direction.

In spinel AlV_2O_4, the presence of multivalent V ions in the pyrochlore lattice of the cubic spinel phase leads to charge frustration that is relieved in the room temperature rhombohedral phase by the clustering of vanadium into a heptamer molecular unit along with a lone V atom. Analysis of X-ray and electron diffraction data shows the formation of a heptamer molecular unit of vanadium ions in AlV_2O_4 as shown in Figure 2c. There are three in-equivalent vanadium sites (V1-yellow, V2-red and V3-blue). In the Heptamer molecular formation V2 is sandwiched between V3 trimers that form the Kagome lattice. Presently ordering of t_{2g} orbitals of vanadium ions is suggested to be the basis of heptamer formation that relieves the frustration. The charge ordering transition in $LiRh_2O_4$ reveals yet another novel scenario which is different from the rest. In fact $LiRh_2O_4$ undergoes a band Jahn-Teller transition associated with a structural transition to tetragonal phase at 230 K. But the charge order transition to a valence bond solid state occurs at 170 K through a further structural transition to an orthorhombic phase. The nature and details of the charge ordering are still poorly understood.

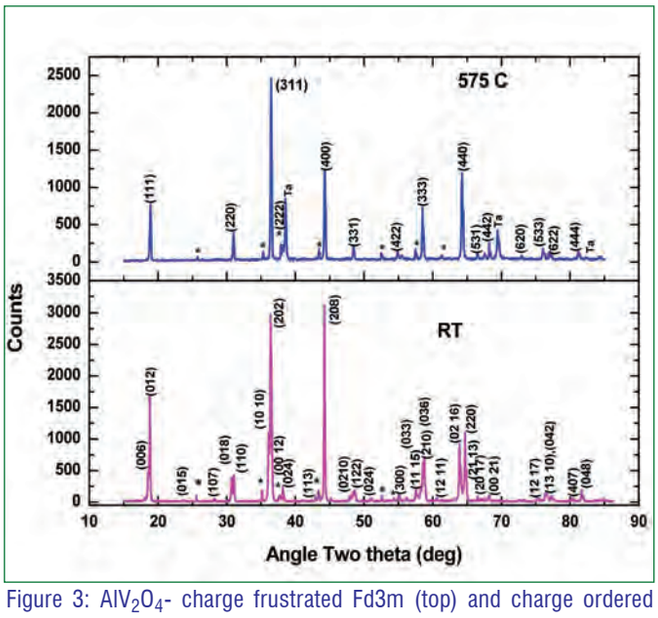

Figure 3: AlV_2O_4- charge frustrated Fd3m (top) and charge ordered R-3m (bottom)

Probing order and frustration in AlV_2O_4

The availability of charge ordered structure at ambient temperature prompted the synthesis of this compound to probe further in to the ordered state. AlV_2O_4 is synthesized in our laboratory using solid state reaction technique in a sealed quartz tube at 1150°C for 150 hours. Ambient temperature powder diffraction data collected using the STOE diffractometer confirmed formation of the heptamer R-3m structure in the charge ordered state. High temperature powder diffraction experiments carried out at various temperatures using the Siemens Diffractometer, confirmed the presence of the cubic frustrated phase around 575°C as shown in Figure 3.

In AlV_2O_4, the charge ordering itself is suggested to be due to the ordering of the t_{2g} orbitals of vanadium ions. It is also known from the literature that partial substitution of Cr for V destroys the ordering. Considering the complexity of the concerned system, it is interesting to experiment on the role of pressure in this system. Therefore X-ray diffraction measurements under high pressure were carried out at beam line 12.2.2 of the Advanced Light Source, Lawrence Berkeley National Laboratory as a collaborative effort. An X-ray wavelength of 0.4959 °A, with a beam size of 10 x10 μm in a symmetric diamond cell with a culet size of 300 μm was used to collect powder diffraction data up to 30 GPa. Variation of unit cell volume as a function of pressure for AlV_2O_4 is shown in

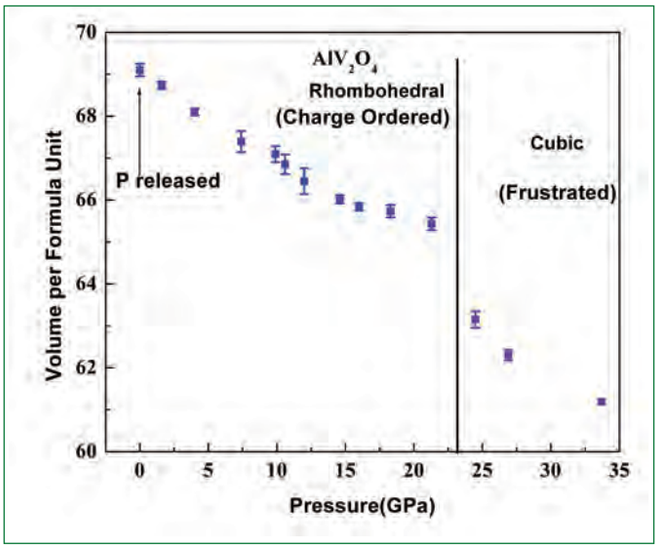

Figure 4: Pressure induced frustration in AlV_2O_4

Figure 4 Up to a pressure of 23 GPa AlV_2O_4 retains the charge ordered state with rhombohedral structure but for pressures beyond, it transforms to the charge frustrated cubic structure. Note that the charge ordered phase appears once again after pressure is released indicating reversiblility of the transition.

The heptamer model for the charge ordered phase of AlV_2O_4 invokes overlap of vanadium orbitals for the formation of charge ordered clusters. These clusters form with a slight readjustment of the position of vanadium in the parent cubic phase. Such a readjustment is reversed on application of pressure, resulting in the modification of orbital overlap and retention of frustration. Further, combining the high temperature and high pressure results, it may be conjectured that there exists a critical range of strain for the planes involving the Kagome lattice of vanadium (V3), beyond which the delicately balanced orbital overlap must be getting inhibited, destroying the heptamer clusters and driving the system back to frustration.

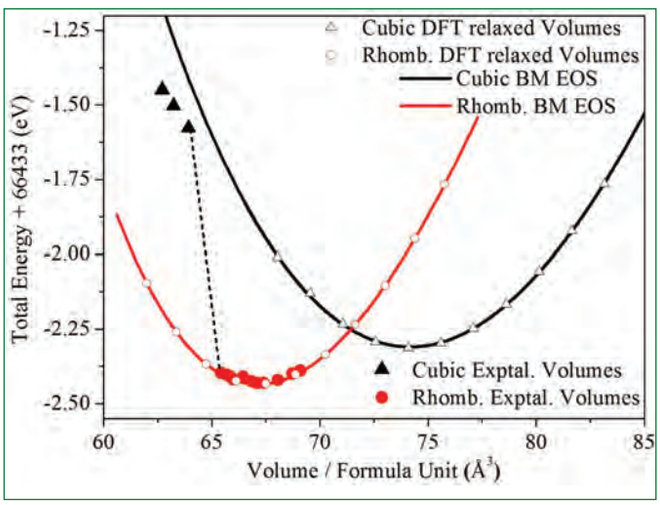

Figure 5: Total energy as a function of volume per formula unit for AlV_2O_4

Ab-initio electronic structure calculations within the density functional formalism have been performed for the charge ordered rhombohedral phase and the charge frustrated cubic spinel phase of AlV_2O_4 to estimate the relevant bulk properties from the total energy. Properties of AlV_2O_4 in both the rhombohedral (R-3m, 166) and cubic spinel (Fd-3m, 227, 2nd setting) structures have been carried out using the full potential linearized augmented plane wave (FP-LAPW) method as implemented in the all electron WIEN2k code. The Wu-Cohen formulation of the generalized gradient approximation (GGA) has been used to estimate the exchange and correlation functionals. Experimental cell parameters under pressure have been used as input to compute the total energy with the same criterion for convergence as follows. For finding the minimum energy structural configuration in the charge ordered rhombohedral phase, the aH and cH/aH ratio have been optimized and then the atomic positions have been relaxed so that the inter-atomic forces between the atoms are less than 5 mRyd/a.u. In the cubic spinel structure, only the lattice parameter needs to be optimized followed by the atomic position relaxation.

Figure 5 shows the results of the computation. The experimental initial volumes are shown by filled circles (rhombohedral phase) and filled triangles (cubic phase) and the relaxed values are shown as open circles (rhombohedral phase) and open triangles (cubic phase). A very good agreement is observed between the experimental and relaxed volumes in the case of the charge ordered rhombohedral phase though such an agreement is elusive in the cubic phase possibly due to the broadening of peaks under pressure. The convergence obtained at lower volumes despite the over estimation of energy corroborates the fact that AlV_2O_4 is driven from charge order to frustration under pressure. Thus the results of computation corroborates the fact that application of high pressure leads to collapsing of the vanadium heptamer sub units and drive the system to frustration. It remains to be seen if pressure would induce frustration in the other charge ordered spinels. Understanding this aspect would require high pressure powder diffraction studies under low temperature down to at least about 150 K.

The physics of charge frustrated spinels in all its complexities can only be comprehended if more systems showing frustration are explored. It is to be identified if the formation of multimer molecular units is at the basis of relieving of frustration and if so, is there a defining stability criterion or, are there going to be situations where the frustration will survive till the lowest of temperature and if it does, what kind of fluctuations can be expected.

S. Kalavathi and colleagues
Materials Science Group

High Fidelity Computational Modelling of Intermediate Heat Exchangers and Steam Generators for Future FBR

The design and analyses activities for the next generation higher power Fast Breeder Reactors (FBR 1&2) have been initiated at IGCAR. Each reactor of FBR 1&2 is a 600 MWe pool type reactor with several innovative improvements with respect to enhanced safety and economy. There are two secondary sodium circuits, each provided with two modules of intermediate heat exchangers (IHX) and three modules of steam generators (SG). Each IHX is of 375 MWt capacity and with 3900 tubes arranged in circular pitch around a central downcomer. Primary sodium enters across the tubes through an inlet window and flows in the shell side before exiting through an outlet window. Secondary sodium flows inside the tubes in counter current direction to primary flow. There are six steam generators of 250 MWt capacity each, having 547 tubes of 30 m length. Seam generators are straight vertical once through type heat exchangers with secondary sodium flowing in the shell side and water/steam flowing in the counter current direction inside the tubes.

To ensure safe mechanical design of these heat exchangers, it is essential to establish thermal loading on the tubes and the shell. The thermal loading occurs due to temperature difference among the tubes and between tube bundle and shell. The differential temperature is caused due to various factors, viz., unfavorable flow distribution of coolants, flow bypassing, cross flow of coolant at the inlet and outlet regions of heat exchangers etc. All these phenomena are associated with multi-dimensional nature of fluid flow and heat transfer and involve conjugate heat transfer by convection and conduction. Therefore, the design tools which are generally based on either lumped model or one dimensional approximation are not capable of addressing the above issues. With the advancement of computational fluid dynamics tools and faster computational resources, these complexities are being addressed by utilizing more realistic computational models. The key challenges involved are need for coupled simulations involving tube side and shell side fluids together and the large number of computational meshes involved. In addition, the heat transfer processes in steam generators involve various regimes of boiling.

Coupled Analysis of Intermediate Heat Exchanger

Figure 1 shows the schematic of IHX, wherein the tubes are arranged in circular pitch surrounding a central down comer. Due to mixed radial and axial flow of primary sodium and counter-current flow of secondary sodium, the tubes are subjected to varying temperatures. These non-uniform temperatures cause

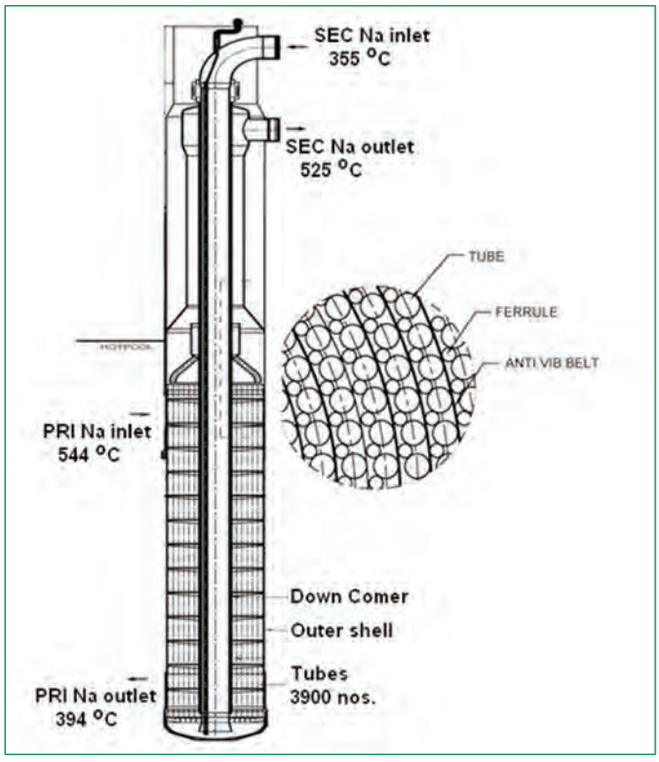

Figure 1: Schematic of intermediate heat exchanger

compressive and tensile loads on the tubes. It is essential to estimate the temperature field in primary and secondary sodium as well as in tubes for estimating the mechanical loading on various structural parts. Generally, tubes in outer rows face hot primary sodium and the temperature of these tubes can be limited by increasing the secondary flow inside these tubes by adopting a suitable flow zoning concept. The pertinent temperature differences can be evaluated by the following analysis methods with increasing accuracy:

(1) Using one dimensional (1-D) hydrodynamic and lumped thermal models combined with networking of parallel channels for tubes and series-parallel paths for shell side flows

(2) Axi-symmetric two dimensional, porous body formulation for the shell side, with heat sinks to simulate heat transferred to the tube side

(3) Using a three dimensional (3-D) model, with explicit representation of the tubes considering the conjugate heat transfer of convection in liquid and conduction through tube walls.

To start with a simplified 1-D network model was developed and analysis was carried out for different secondary side

flow zoning options. The case of 30% more flow in the outer 7 rows was found to be acceptable from the point of view of minimum thermal loading. Subsequently, this flow zoning was evaluated using the third method stated above. This required a three dimensional 60° sector model of IHX with convection in primary and secondary sodium coupled with conduction in tube walls (Figure 2). The number of computational meshes in the 3-D model was 2.9 million (Figure 3). The computational time for one steady state simulation was 6 days in a four core CPU.

The flow and temperature distributions of primary sodium in the shell side and secondary sodium inside tubes have been solved as a conjugate problem. Velocity inlet boundary conditions are used for primary and secondary sodium flows. Specification of primary sodium inlet velocity helps in decoupling the IHX from the hot pool. Values of inlet velocity in various tubes are arrived at from the parametric studies carried out using the 1-D network model. Pressure outlet boundary condition with constant pressure is imposed on the primary and secondary outlets. The anti-vibration belts are modeled using a porous body model, wherein the pressure drop due to anti-vibration belts is specified as momentum sink in the axial momentum balance equation. This helped in reducing the computational effort without

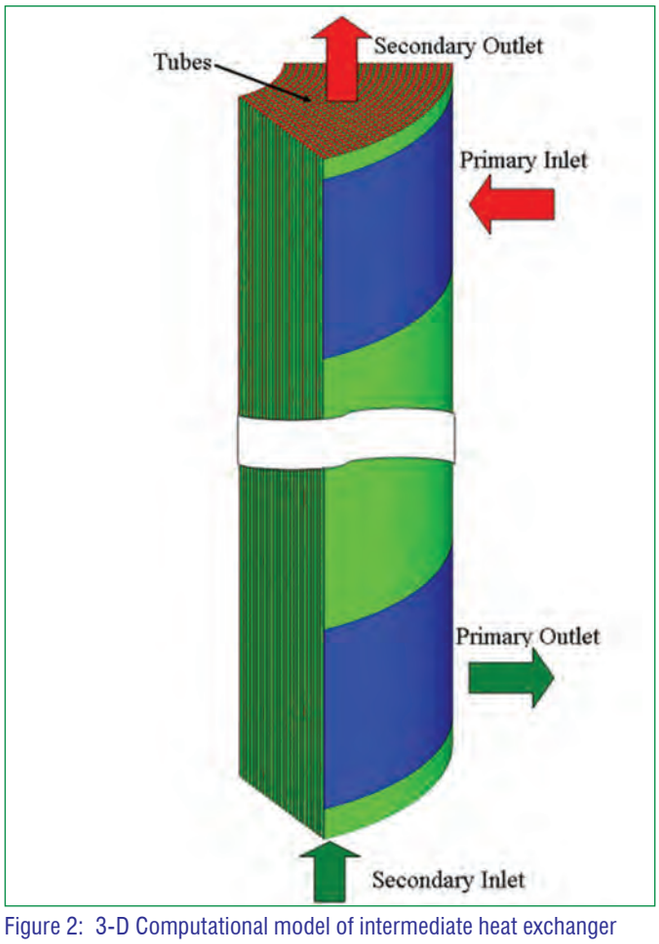

Figure 2: 3-D Computational model of intermediate heat exchanger

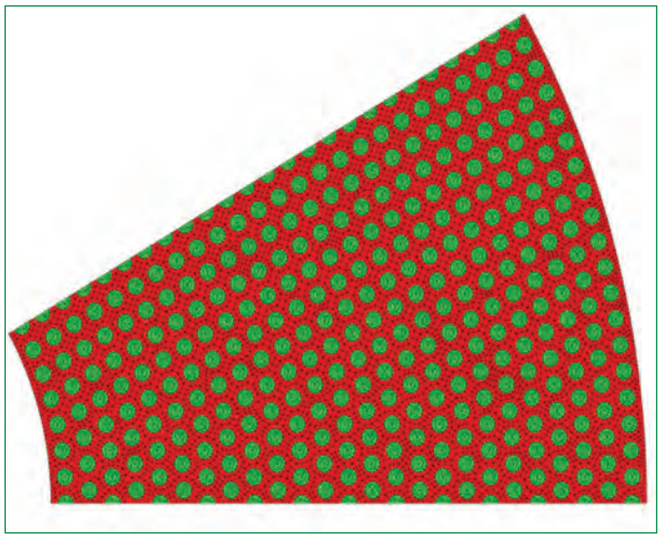

Figure 3: Computational mesh of intermediate heat exchanger

significantly compromising on the accuracy of the results. High Reynolds number version of k-ε turbulence model with standard wall function has been used for modeling turbulence. The well-known SIMPLE algorithm is used for handling pressure-velocity coupling. Effect of buoyancy on sodium flow distribution in primary and secondary sides is modeled by Boussinesq approximation.

From the predicted 3-D velocity distribution, it was found that the primary sodium flow is radial near inlet while at the outlet window the radial flow is superimposed with a large axial velocity component. In the remaining regions the flow is predominately axial. Due to the 90° axial turn of primary sodium near the inlet window, the regions near tube rows adjacent to the inner shell receive low primary sodium flow. Such effects are not predictable from 1-D models.

Figures 4 and 5 depict the temperature of secondary sodium at the outlet with uniform secondary flow and 30% more secondary

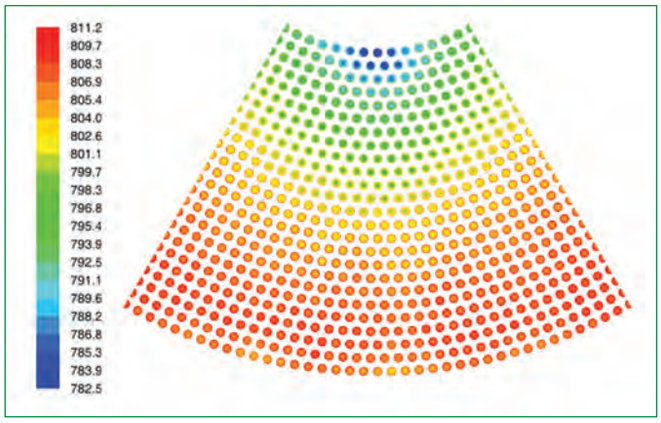

Figure 4: Temperature (K) contours of secondary sodium at intermediate heat exchanger outlet without flow zoning

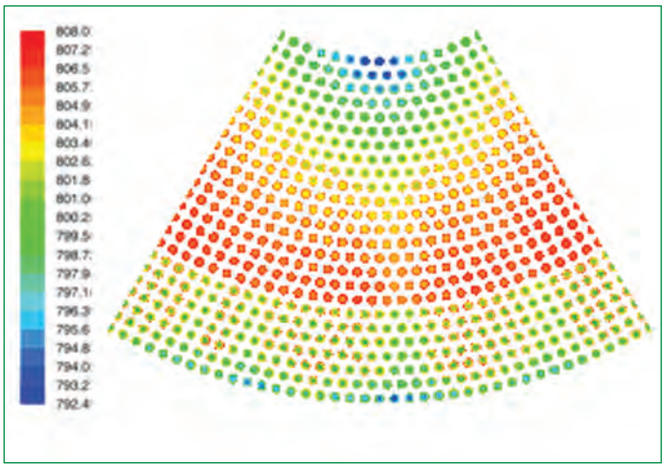

Figure 5: Temperature (K) contours of secondary sodium at intermediate heat exchanger outlet with flow zoning

flow in the outer 7 rows of tubes respectively. The temperature contours exhibit a clear distinction because of flow zoning. The effect of flow zoning on the primary sodium was found to be limited to the outer few rows.

From the primary sodium flow field at the outlet window a dead zone of ~ 0.3 m was observed near the top surface of bottom tube sheet. The axial variation of average temperature of primary sodium at the outlet window along the height exhibited a temperature difference of 62°C. This value decreased to 46°C when flow zoning was adopted.

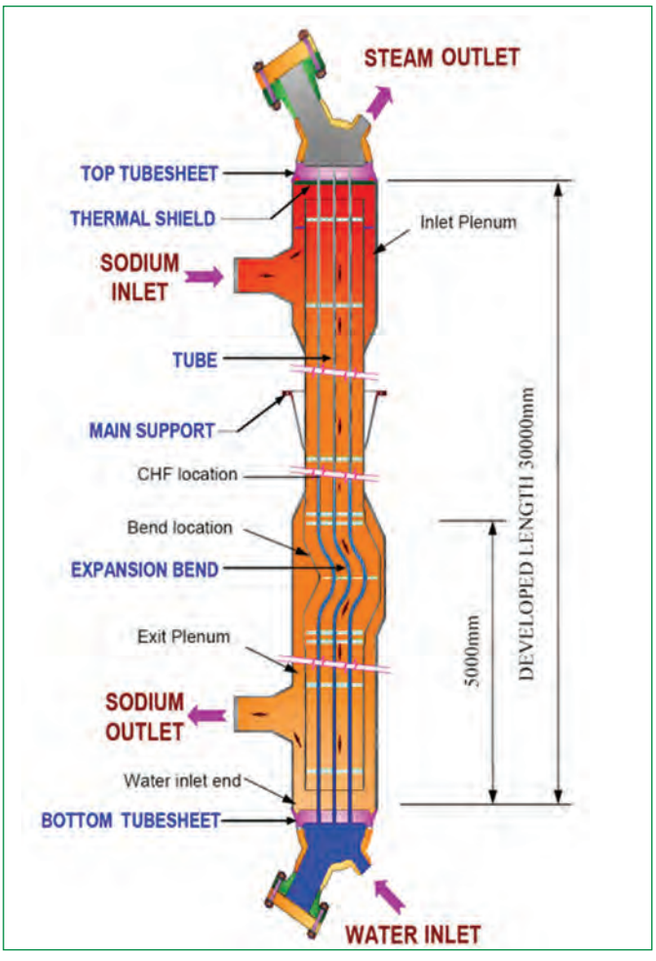

Figure 6: Schematic of steam generator

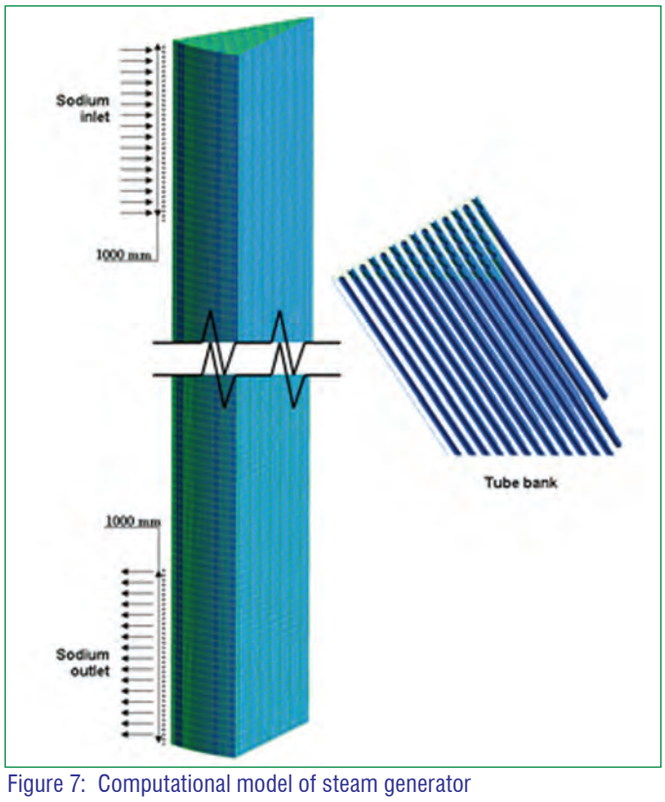

Figure 7: Computational model of steam generator

A difference of 25°C was observed in the secondary sodium temperature at the outlet in the reference design without flow zoning. This value decreased to 14°C with flow zoning. Buckling ΔT (temperature difference between hottest tube and tube bundle average) of 5°C was observed in the reference case. This value marginally increased to 9°C with flow zoning. Similarly, the pull-out ΔT (temperature difference between tube bundle average and coldest tube) of 9°C in the reference case marginally increased to 17°C with flow zoning. The power transferred as predicted by the 3-D coupled model was 385 MW and 383 MW for both the cases. These values are greater than the design value of 375 MW suggesting that the margin provided in the process design is adequate to account for the 3-D effects. Based on the investigations of two options, flow zoning concept with 30% more flow in outer 7 rows of tubes is recommended for design and it is expected that the thermal loading affecting the life of IHX is significantly reduced.

Coupled Analysis of SG

Schematic of steam generator is shown in Figure 6. A coupled code approach is adopted for the detailed analysis of SG.

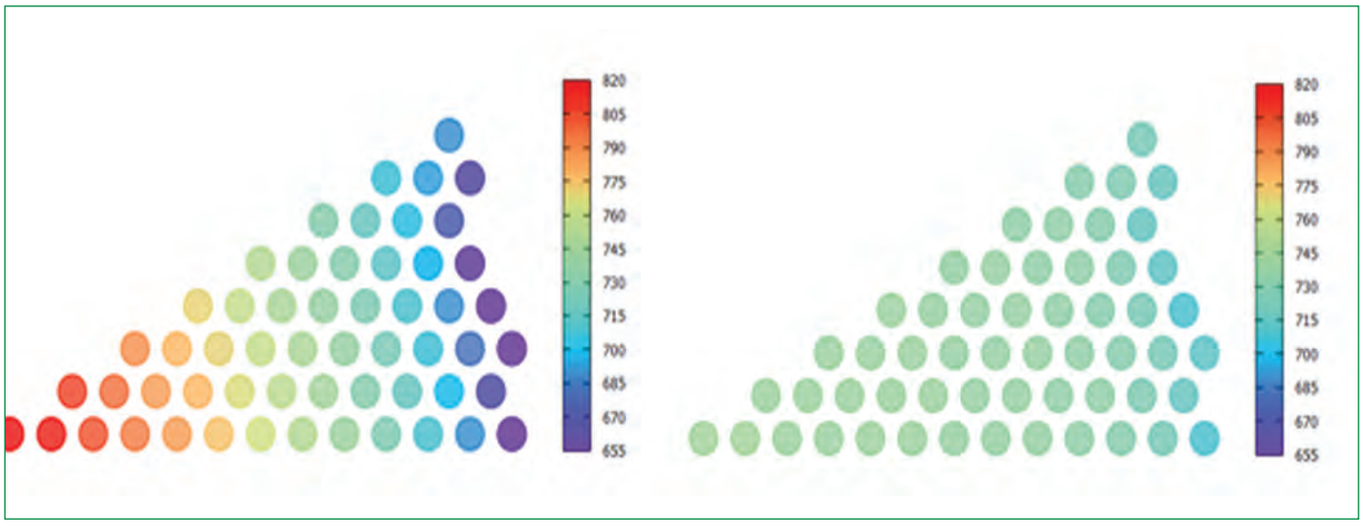

Figure 8: Water flow rate (kg/h) variation among the tubes of SG for cases 1 (left) and 2 (right)

This is mainly due to the difficulties in the simulation of phase change phenomena occurring in the tube side of SG. Flow and temperature distributions of sodium on the shell side of the SG are simulated using the CFD code, while the tube side pressure drop, flow distribution and heat transfer in all the flow regimes are modeled, using the one dimensional code DESOPT. The coupling of CFD software with the DESOPT is established through a set of user subroutines. A water flow correction subroutine is also coupled to maintain same tube-side pressure drop amongst all the tubes. Each SG consists of 547 tubes, which are arranged in a triangular pitch. A 30° sector of SG (see, Figure 7) is considered for the multidimensional CFD analyses. This sectoral domain consists of 56 tubes, of which 19 are half tubes, 36 are full tubes and the central tube is one-sixth. Wall thickness of tubes, is also modeled explicitly. The computational domain is discretized into 3 million hexahedral elements. Sodium inlet boundary is supplied with uniform mass flow boundary condition, while sodium outlet is considered as constant pressure outlet condition. The tube inner walls have been specified with temperature boundary condition and the corresponding temperature values are fetched from DESOPT. The pressure drop encountered by sodium flow at the tube support locations is accounted by porous jump approximation. Standard high Reynolds number k-ε model with wall function approach is deployed to account for turbulence.

Before adopting the model to prototype SG, it was used to simulate the 5 MWt Steam Generator Test Facility (SGTF) with 19 tubes. The predicted results of steam outlet temperature, pressure drop in tubes, power transferred in the SG were compared with the measured data. A satisfactory agreement was noticed validating the computational model and its suitability for prototype SG. Subsequently, 3 different cases have been analysed to elucidate the flow and thermal characteristics in the prototype SG. In case-1, the tie rods, which are used for holding bundle supports, are not considered. It may be highlighted that each tube is provided with an orifice at the inlet to eliminate flow instabilities in the Once Through Steam Generators. These orifices offer a pressure

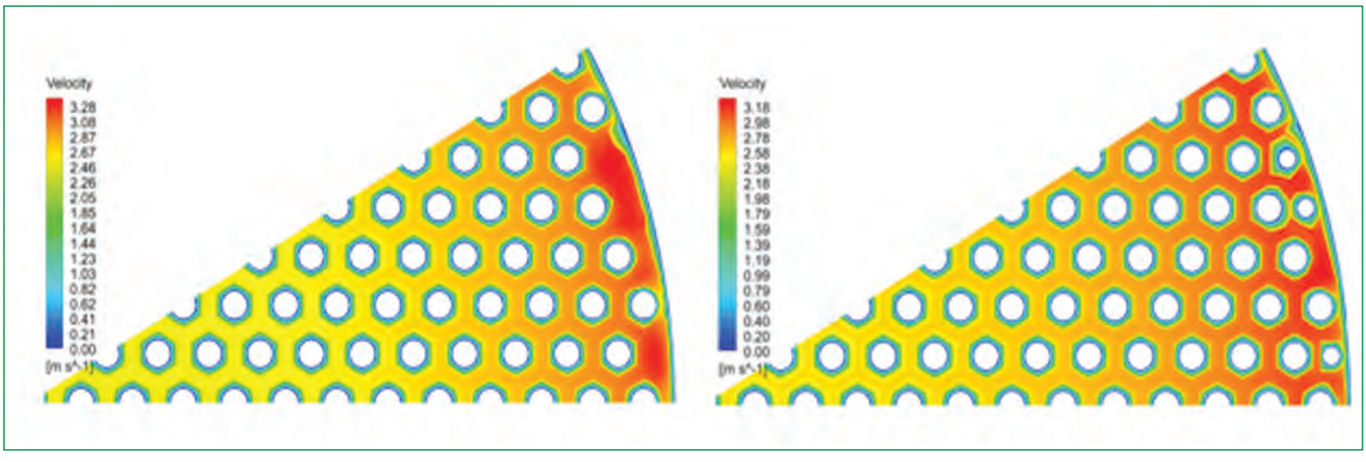

Figure 9: Sodium velocity magnitude (m/s) contours in Z = 1m plane of SG for Cases 2 (left) and 3 (right)

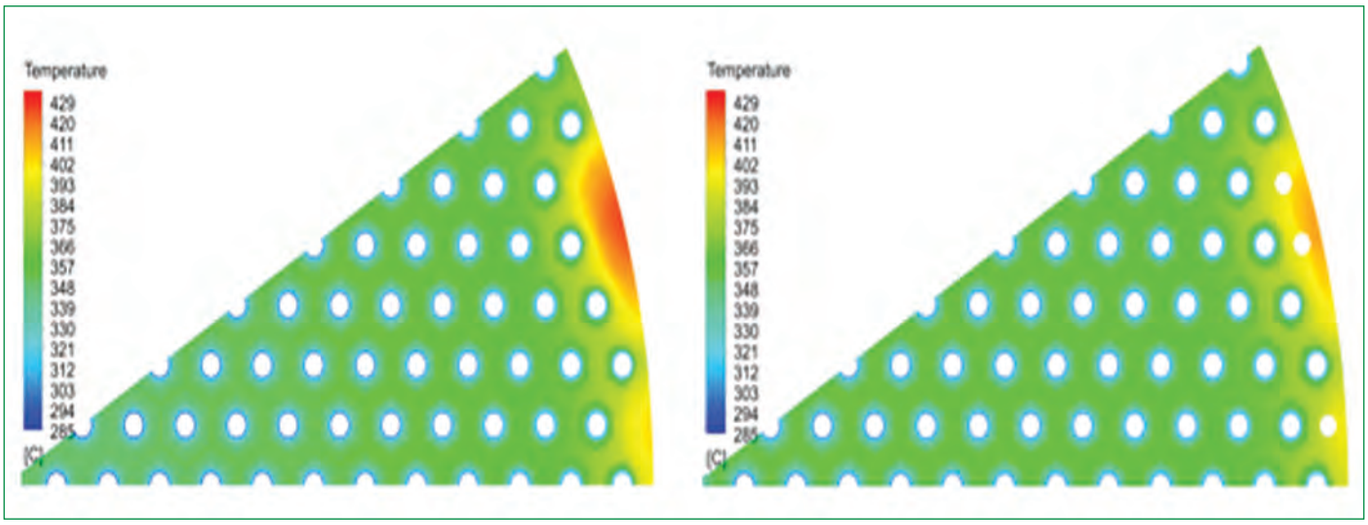

Figure 10: Sodium temperature (°C) contours in Z = 1m plane of SG for Cases 2 (left) and 3 (right)

drop of ~1 MPa. The influence of this orifice pressure drop on the flow correction in each tube is not accounted in case-1. In case-2, the influence of orifice pressure drop is accounted. In case-3, in addition to orifice pressure drop, three tie rods are considered and modeled in the 3-D simulations.

The predicted sectional velocity contours of case-1 indicate that there is significant flow bypass near the shell. The velocity of flow in the bypass regions is about 10% greater than that in the central region. This causes significant temperature variation across the section. Further, it is found that there is a significant variation in water flow rate from 655 to 820 kg/h (Figure 8) among the tubes which is caused due to the sodium flow distribution. The steam temperature at the exit is found to vary from 468 to 519°C. When orifice offering 1 MPa pressure drop is added to the tubes, the variation in water flow among the tubes significantly reduced (709 kg/h in the outermost tube and 745 kg/h in the central tube) as depicted in Figure 8. The steam temperature variation is also narrowed down to 23°C with the help of orifices. Predicted sectional sodium velocity contours for case-2 (Figure 9) are similar to case-1. But the sectional temperature contours for case 2 show that the sodium temperature distribution is nearly uniform in the central tube bundle region except in the region close to the outer rows where there is significant flow bypass (Figure 10).

The option of eliminating bypass flow of sodium near the shell side is examined by inserting three tie rods (case - 3). Contours of sodium velocity magnitude at Z = 1 m plane (above the bottom tube sheet) in cases 2 and 3 are depicted in Figure 9. This indicates that the insertion of tie rods helps in reducing the bypass flow velocity near the shell. Though the insertion of tie rods bring down the sodium velocity in the vicinity of shell, the temperature contours depicted in Figure 10 show that high sodium temperature prevailing in this region cannot be completely eliminated. More uniformity in water flow rate is also achieved by the insertion of tie rods which is attributed to uniformity in the heat absorbed among the tubes. Also, due to the better flow uniformity in the tube side, the exit steam temperature variation reduces to 19°C. The maximum difference between the tube bundle average temperature and the hottest tube are 31, 22 and 18°C respectively for first, second, and third cases. Similarly, the difference between the average temperature of tube bundle and shell are 78, 71 and 65°C respectively for these cases. Thus, the orifice offering 1 MPa pressure drop in the tube side and tie rods in the shell side significantly reduce the thermal loading on the structural parts of SG.

A series of network based 1-D model and high fidelity 3-D CFD model have been developed for thermal hydraulic analyses of heat exchange equipment. The conjugate CFD model for SG has been validated against the data measured in SGTF. Following these, three dimensional analyses for IHX and SG of future FBR have been carried out. These analyses provided detailed information regarding the flow and thermal features within the heat exchange equipment. It is very difficult to measure such intricate flow physics in experiments due to the limitations in instrumentation. Based on the analyses the secondary sodium flow zoning concept for IHX and the tie rod as well as orifice pressure drop for SG have been finalized to achieve the design targets.

P. Puthiyavinayagam and colleagues
Reactor Design Group

Young Officer's FORUM

Tri-iso-amyl Phosphate: A Potential Extractant for the Reprocessing of Spent Nuclear Fuels

A solution of TBP diluted with n-alkane diluents (1.1M) has been utilized as a versatile solvent in various separation processes and for the reprocessing of thermal and fast reactor fuels (PUREX process). However, the experience gained in the past several decades has revealed few drawbacks that are of concern in various separation processes. The main limitations of TBP are a) its relatively higher solubility in aqueous media b) third phase formation with tetravalent metal ions such as Pu(IV), Th(IV), Zr(IV) c) its vulnerability towards chemical and radiolytic degradation etc.

Third phase formation is an important phenomena which must be considered while designing flow sheets for the processing of spent nuclear fuels. This is particularly important for fast reactor fuel reprocessing, due to the presence of high plutonium content. Earlier, several symmetrical trialkyl phosphates have been investigated in our laboratory towards the identification of an alternate extractant to TBP for fast reactor fuel reprocessing and identified that tri-iso-amyl phosphate (TiAP) is a potential extractant for the fast reactor fuel reprocessing. In addition to its excellent extraction behaviour and high capacity to load Pu(IV) without third phase formation, it has lesser aqueous solubility (< 80 mg/L) as compared to TBP. The chemical structures of TiAP and TBP are shown in Figure 1.

The feasibility of using TiAP for actual reprocessing applications has been demonstrated by conducting various studies and results are presented in this report.

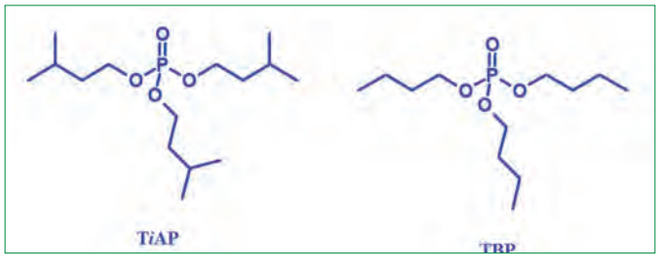

Figure 1: Chemical Structures of TiAP and TBP

Dr. Balija Sreenivasulu joined Fuel Chemistry Division, Indira Gandhi Centre for Atomic Research in the year 2010 after completing OCES from 4th batch of BARC training school, IGCAR campus. He Obtained his M.Sc. from University of Hyderabad and Ph.D from HBNI. He has been adjudged as the winner of the young innovator challenge during FR17, Yekaterinburg, Russia organised by IAEA. He is also the recipient of "young applied scientist/ technologist award" for the year 2016 for his outstanding contributions. His main areas of interest are development of alternate extractants for fast reactor fuel reprocessing, aqueous reprocessing of metal fuels and solvent extraction and extraction chromatographic studies. He has twelve peer reviewed journal and fifteen symposium publications.

Extraction of U(VI) and Pu(IV) with TiAP from nitric acid media

Studies on third phase formation with Pu(IV)-HNO_3–TBP system were reported in literature. However, similar studies with high plutonium concentration have not been carried out with TiAP. In this context, the extraction of Pu(IV) by 1.1M TiAP/DD from plutonium nitrate solution(72-283 g/L) has been investigated. The variation of $D_{Pu(IV)}$ with $[Pu(IV)]_{aq,eq}$ for various concentrations of nitric acid is shown in Figure 2. These studies indicate that $D_{Pu(IV)}$ initially decrease steeply and flatten with increase in $[Pu(IV)]_{aq,eq}$ at 2M, 4M and 6M HNO_3. However, in the case of 0.5 M HNO_3, $D_{Pu(IV)}$ initially increase and then decrease. It was reported that in the case of Pu(IV)-1.1M TBP/DD-HNO_3 system, tendency for third phase formation was higher at 2M HNO_3, whereas in the case of TiAP system, third phase formation was not observed even at

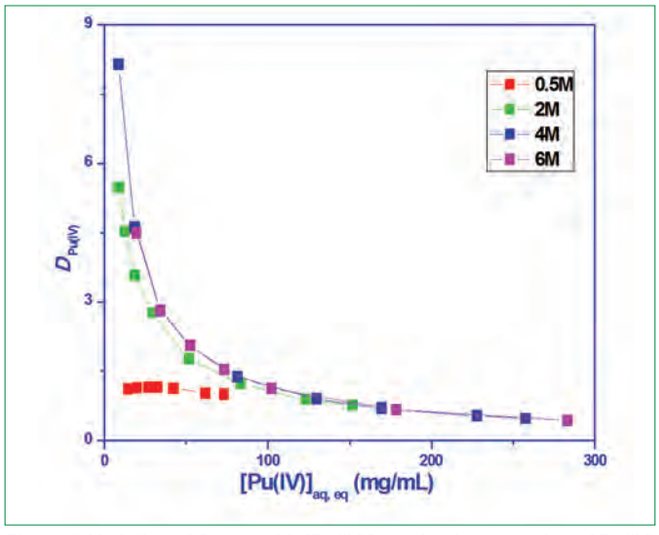

Figure 2: Variation of $D_{Pu(IV)}$ with $[Pu(IV)]_{aq,eq}$ for the extraction of Pu(IV) by 1.1M TiAP/DD from plutonium nitrate solutions in nitric acid media at 303 K

this acidity. These studies indicated that TiAP can be employed for reprocessing of plutonium rich fuels.

Co-processing of U(VI) and Pu(IV) which involves the recovery of Pu along with U results in resistance to nuclear proliferation and reduces the cost of the process by avoiding Pu partitioning cycle and Pu purification cycle. Prior to continuous counter-current solvent extraction runs with high metal loading conditions using a mixer-settler facility, batch studies are carried out in cross-current mode to assess the number of stages required for the co-extraction and co-stripping of heavy metal ions using 1.1M TiAP/DD system. The concentrations of feed solution are chosen to simulate the dissolver solution of PFBR MOX fuel (28% initial Pu) with a burnup of 10 atom% fission. The concentrations of U(VI) and Pu(IV) in the feed solution were about 254 g/L and 64 g/L, respectively in 4M HNO_3.

The flowsheet for the co-extraction and co-stripping of U(VI) and Pu(IV) by 1.1M TiAP/DD in cross-current mode is shown in Figure 3.

The maximum loading of U(VI) and Pu(IV) in the organic phase was found to be 106 and 20.9 g/L, respectively, in the 1st stage of cross-current extraction. The concentration of Pu(IV) in the aqueous phase (raffinate) in the 4th stage was below detection limit (BDL) which is less than 0.002 g/L, whereas U(VI) concentration was around 0.14 g/L. Subsequently, stripping of the metal ions from the organic phase was carried out using 0.35M HNO_3. Most of the Pu(IV) was stripped within the two stages whereas stripping of U(VI) was observed in all the four stages. The concentrations of U(VI) and Pu(IV) in the organic phase (lean organic) after 4 stages of stripping were 15 and 3.2 g/L, respectively.

The extraction behaviour of fission product elements:

The extraction behaviour of Zr(IV), RuNO(III), TcO_4^-, Lns and Am(III) with 1.1M solutions of TiAP in *n*-dodecane from nitric acid (0.1–6M) media has been investigated. Results indicate that the $D_{Zr(IV)}$ increases with increase in nitric acid concentration, whereas the $D_{RuNO(III)}$ initially increase up to 1.5M HNO_3 and then decrease

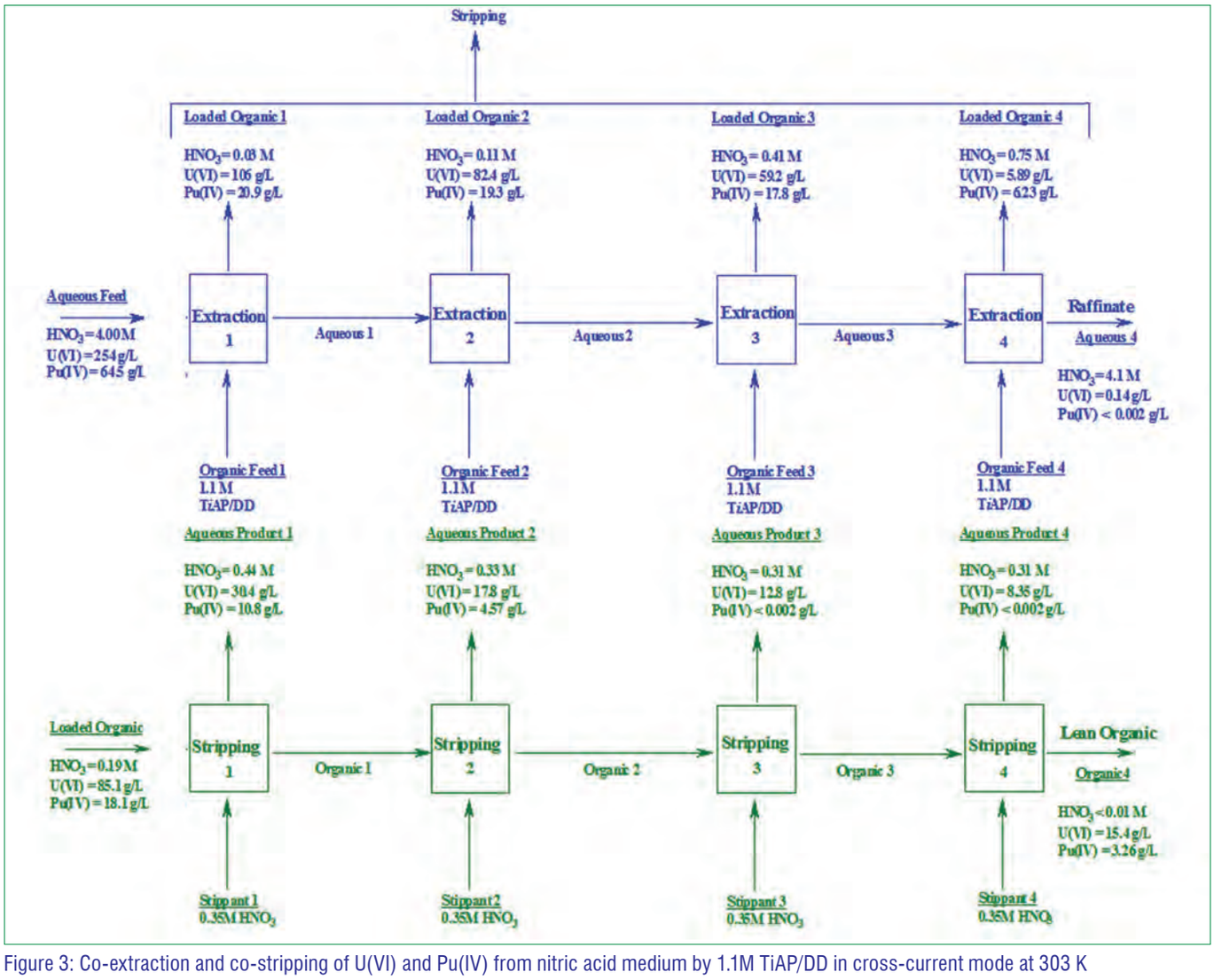

Figure 3: Co-extraction and co-stripping of U(VI) and Pu(IV) from nitric acid medium by 1.1M TiAP/DD in cross-current mode at 303 K

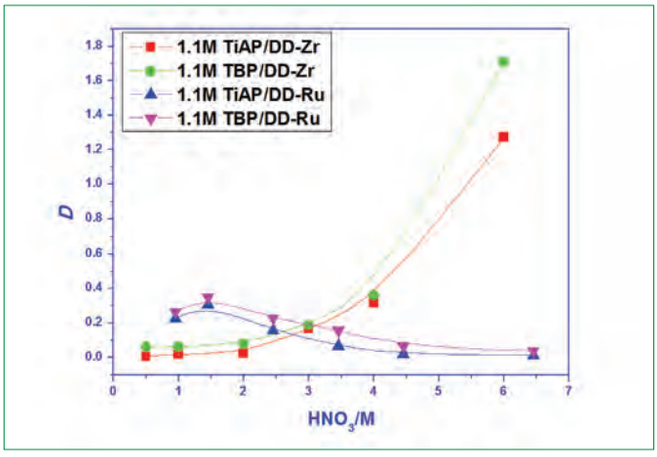

Figure 4: Variation of D as a function of equilibrium nitric acid concentration

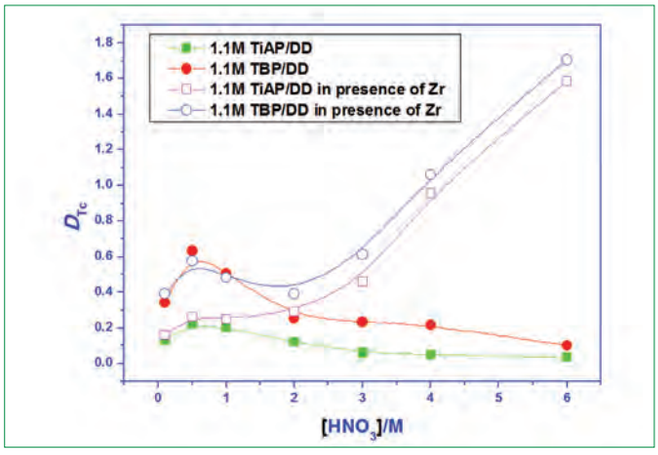

Figure 5: Variation of D_{Tc} as a function of nitric acid concentration

with increase in nitric acid concentration (Figure 4). Extraction data shown in Figure 4, clearly indicates that the *D* values for the extraction of Zr(IV) and RuNO(III) with TiAP are marginally lower than that of TBP, which in turn indicates the possibility of achieving higher decontamination factors with TiAP based solvent.

Like ruthenium, the D_{Tc} first increases up to 0.5M HNO_3 and then decreases with nitric acid concentration (Figure 5). The initial increase in D_{Tc} can be attributed to the formation and extraction of pertecnetate, $HTcO_4$, as the extractable species with increased nitric acid concentration. The extraction behaviour of Tc in presence of Zr has been investigated and the results indicate that the extraction of Tc in presence of Zr is similar to the trend observed as in the case of pure Tc at lower nitric acid concentration (0.1-1M). However, the extraction of Tc by TBP and TiAP increases as the nitric acid concentration in aqueous phase increases and this trend can be seen in the acidity range of 2-6M (Figure 5).

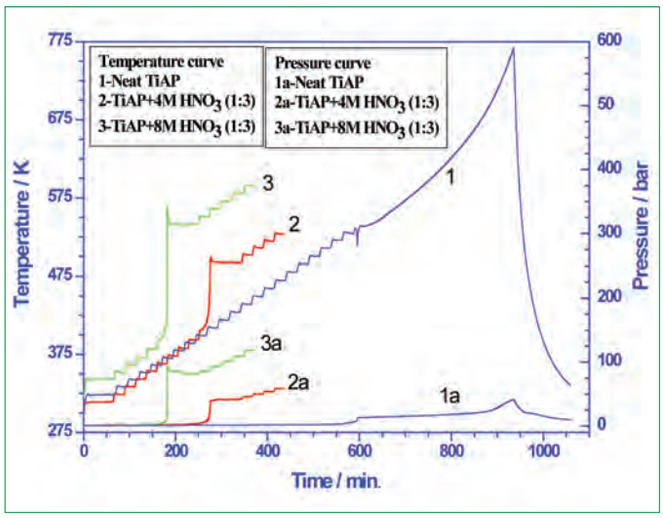

Figure 6: Plot of temperature and pressure vs time for the decomposition of 1) Neat TiAP, 2) TiAP-4M HNO_3 (1:3) and 3) TiAP-8M HNO_3 (1:3)

Degradation studies with TiAP

Radiolytic stability of a solvent is an important parameter to be qualified for the processing of the spent nuclear fuels. The densities of 1.1 M solutions of TiAP and TBP in n-dodecane do not change significantly, whereas their viscosities increase as a function of gamma absorbed dose. IFT values for unirradiated TiAP-HNO_3 system is higher than that of irradiated TiAP-HNO_3 system and IFT values for TiAP-HNO_3 systems are marginally higher than that of TBP-HNO_3 systems.

The effect of α-degradation on TiAP and TBP was studied by loading Pu(IV) into the organic phase and measuring the amount of Pu retained in the organic phase after stripping with nitric acid. The Pu retained in the organic phase was stripped as a function of time; the loaded organic phase was found to contain ~12 mg/L Pu at zero hours of contact time and it was ~600 mg/L when Pu loaded organic phase was kept for 424 h followed by stripping. The retention of Pu in the organic phase increases with increase of absorbed dose. The Pu retention by 1.1M TiAP/DD and 1.1M TBP/DD is nearly comparable under identical conditions, indicating that the degradation behavior could also be similar.

Figure 7: Mixer-settler facility used for flow sheet development studies

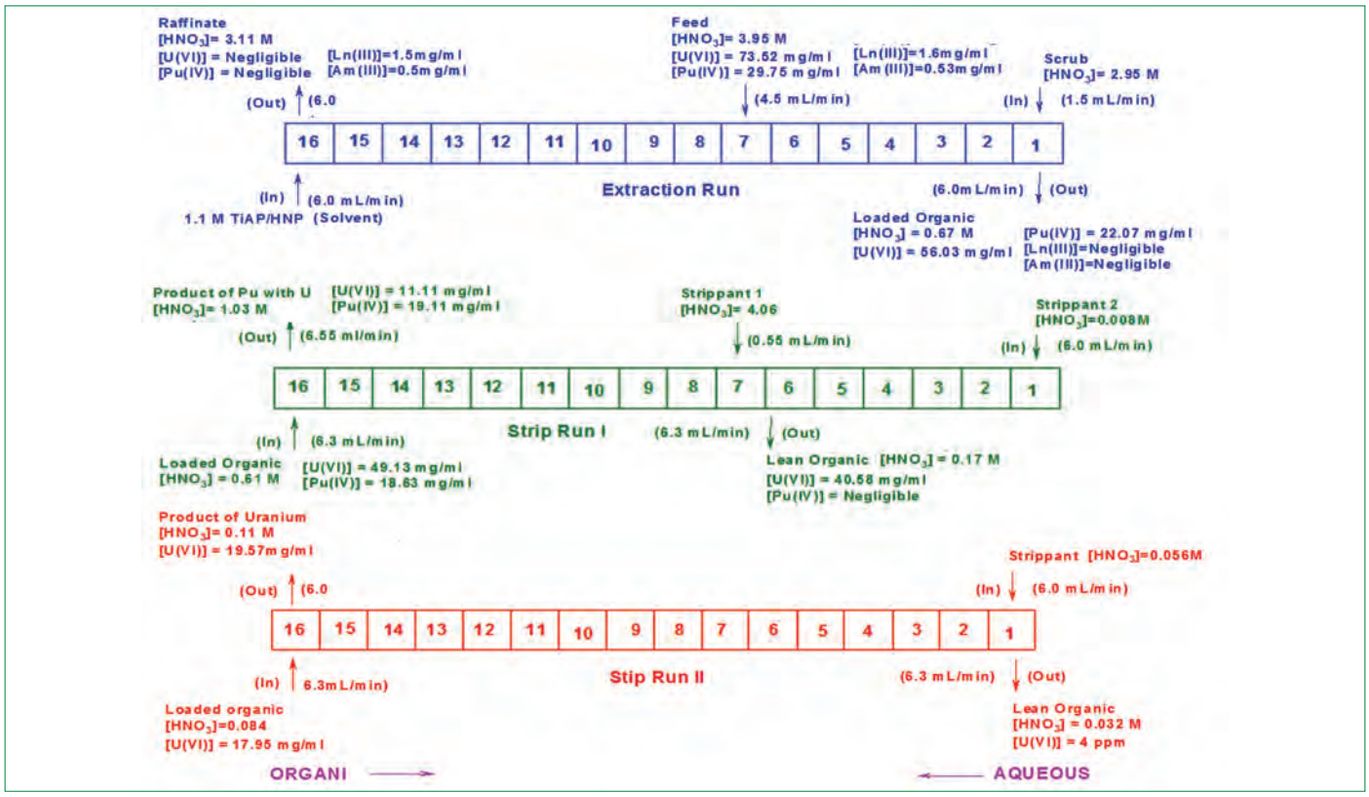

Figure 8: Flow sheet for the separation of U(VI) and Pu(IV) from Am(III) and Ln(IIII) by 1.1M TiAP/HNP

The thermal decomposition behaviour of TiAP–HNO_3 biphasic (organic and aqueous phases) systems was investigated using an adiabatic calorimeter. Experiments were conducted in a closed air ambience under heat-wait-search (H-W-S) mode. These studies established that neat (unirradiated) TiAP is stable up to 540 K and above this temperature; it undergoes exothermic decomposition, whereas the irradiated TiAP exhibits decomposition beyond 490K in the absence of nitric acid. However, in the presence of nitric acid, TiAP decomposes at much lower temperature (384-499K) with formation of incompressible gases and viscous black liquid (Figure 6).

Mixer-settler runs with TiAP under process conditions

A mixer-settler facility consisting of an ejector mixer-settler unit and valve-less metering pumps housed in a double-module glove box has been commissioned in our laboratory (Figure 7). In order to understand solvent recycling and decontamination factors achievable in TiAP system, the solvent used in the earlier runs has been recycled to perform mixer-settler runs for the demonstration of the bulk separation of U(VI) and Pu(IV) from Ln(III) and Am(III). An aqueous feed solution containing ~30 g/L of plutonium, ~70 g/L of uranium, ~ 0.53 g/L of Am(III) and ~ 1.6 g/L of lanthanides (La, Pr, Nd, Sm and Eu) in 4M HNO_3 has been employed.

The basic flow sheet for the extraction and stripping of U(VI) and Pu(IV) comprises of three runs as shown in Figure 8. First run was performed for the separation of U(VI) and Pu(IV) from Ln(III) and Am(III) and the other two runs for the stripping of extracted metal ions from loaded organic phase. Separation of U and Pu from fission products using mixer-settler facility comprising of 16 stages for extraction-scrubbing and 2x16 stages for heavy metal stripping indicates that loss of heavy metals into the raffinate and lean organic streams has been negligible. The flowsheet developed in the present study will be useful for the deployment of TiAP for actual reprocessing applications.

These studies reveal that TiAP based solvent does not form third phase during the extraction of Pu(IV) from nitric acid media. Co-extraction of U(VI) and Pu(IV) by TiAP indicate that it is possible to achieve maximum loading in the organic phase without any phase splitting. These studies also indicate that the extraction behaviour of fissions products by TiAP is comparable to that of TBP and the radiolytic degradation behaviour of TiAP is not very much different from that of TBP. The lower aqueous phase solubility of TiAP has a great advantage in minimising runway reactions. Based on these studies it can be concluded that it is possible to employ TiAP as an alternate extractant to TBP for fast reactor fuel reprocessing.

Balija Sreenivasulu
Materials Chemistry & Metal Fuel Cycle Group

Young Researcher's FORUM

Room Temperature Ionic Liquids (RTILs) for Solvent Extraction and Electrochemical Studies of Lanthanides and Actinides

Dr. R. Rama did her Masters in Applied Chemistry from National Institute of Technology (NIT), Trichy. She joined IGCAR as a Junior Research Fellow in Chemical Sciences in July 2012 and carried out her doctoral work in Materials Chemistry and Metal Fuel Cycle Group, under the guidance of Dr. M. P. Antony. Her doctoral thesis is on "Solvent Extraction and Electrochemical studies of Lanthanides and Actinides in room temperature ionic liquid medium containing various extractants".

Room temperature ionic liquids (RTILs) are composed fully of dissociated ions and their melting points are below 100˚C. RTILs have been receiving increased attention for possible applications in the area of nuclear fuel reprocessing and waste management owing to their remarkable properties. Essentially, RTILs are investigated as possible substitutes to the molecular diluents (for example n-dodecane (n-DD)) in solvent extraction procedures. Moreover, the properties of RTILs such as wide electrochemical window, solubility of various extractants and unusual extraction of target metal ions from aqueous medium etc., facilitates the development of a novel and environment benign procedures for the treatment of wide variety of aqueous wastes using ionic liquid as medium. One such method is the extraction-electrodeposition (EX-EL) approach. Some of the striking features of RTILs that make them promising for nuclear fuel cycle application are (i) selectivity of target metal ion can be easily manipulated by the change of cation-anion combinations of RTIL diluent, rather than redesigning the structure of the extractant (ii) presence of ionic diluent in organic phase facilitates a new mode of recovery of metals by direct electrodeposition from the extracted phase (iii) ionic liquids can be functionalized with organic moieties for task specific applications (iv) RTILs can be designed to be completely incinerable, which would simplify the management of spent organic waste (v) due to negligible vapor pressure of RTILs, the fire hazard is almost insignificant. Superior extraction of target metal ion can be obtained by RTILs system due to the ionic nature and solvating capability of the ionic liquid.

In view of these advantages, we have explored RTIL as diluent, extractant and electrolytic medium for the solvent extraction and electrochemical studies of lanthanides and actinides. The structure of RTILs and functionalized ionic liquid (FIL) developed in our laboratory are shown in Figure 1.

RTIL AS DILUENT:

Mutual separation of Pu(IV) from other actinides

Plutonium Uranium Reduction Extraction (PUREX) process has been in vogue, worldwide, for the recovery of uranium and plutonium from the spent nuclear fuel. This process uses a solution of 1.1 M tri-n-butylphosphate (TBP) in n-DD for the separation of U(VI) and Pu(IV) from the spent nuclear fuel dissolver solution (3–4 M nitric acid). The dissolver solution of thermal reactor fuel is essentially composed of U(VI) in nitric acid medium, as the fuel for thermal reactor is uranium oxide. It also contains small amounts of transuranium elements, fission products and corrosion products. However, the situation is quite different when dealing with fast reactor dissolver solution. In this case, plutonium is the

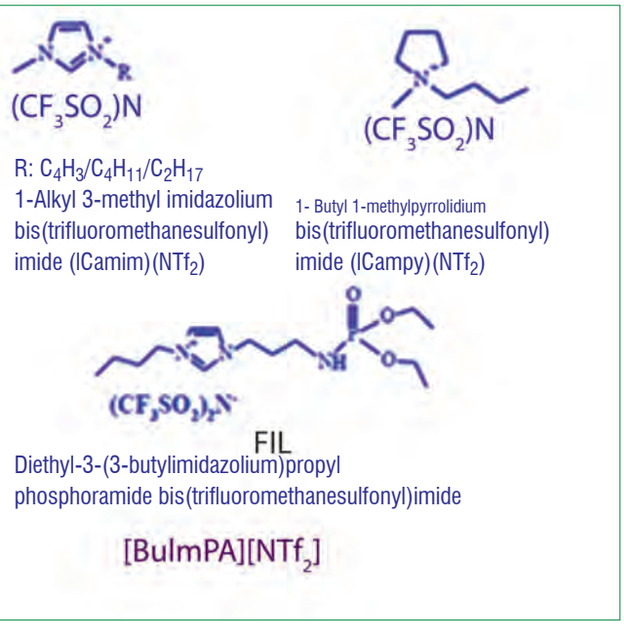

Figure 1: Structure of RTILs and FIL used in the present study

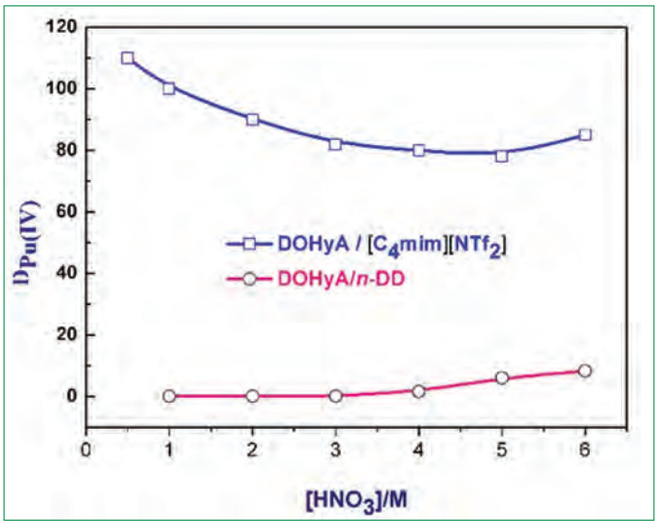

Figure 2: Variation in the distribution` ratio of Pu(IV) obtained in DOHyA/$[C_4mim][NTf_2]$ and DOHyA/n-DD as a function of the nitric acid concentration in aqueous phase

major constituent of dissolver solution as the fuel for fast reactor is $Pu_xU_{1-x}C$ or $Pu_xU_{1-x}O_2$ (x= 55 or 70) and the third phase formation tendency of Pu(IV) and Zr(IV) (fission product) in TBP/n-DD, hydrolytic and radiolytic degradation of solvent pose interesting challenges to separations. Moreover, the separation factor U(VI) over Pu(IV) is less than 2 in TBP/n-DD. In order to overcome the issues associated with the third phase formation of Pu(IV) and improve the separation factor, it is essential to identity alternate solvents for the separation of Pu(IV) from the fast reactor dissolver solution with high separation factor over U(VI). In the recent past, CHNO based extractants are considered as promising candidates for the extraction of actinides due to their completely incinerable property. In the present study, the extraction behavior of Pu(IV) was investigated using 0.02 M N, N-dioctyl-2-hydroxyacetamide (DOHyA) dissolved in RTIL diluent. The results were compared with DOHyA/*n*-DD. Superior extraction

Table 1: Separation factor of Pu(IV) over U(VI) and Am(III) achieved using 0.02 M DOHyA/$[C_4mim][NTf_2]$

$[HNO_3]$/M	Separation factor of actinides in 0.02 M DOHyA/$[C_4mim][NTf_2]$		
	$SF_{Am(III)/U(VI)}$	$SF_{Pu(IV)/Am(III)}$	$SF_{Pu(IV)/U(VI)}$
0.5	38	48	1833
1	20	50	1000
2	7.2	50	360
3	1.9	82	152
4	0.79	127	100
5	0.22	354	78

Table 2: Comparison of separation factor of Pu(IV) over U(VI) obtained in 0.02 M DOHyA/ $[C_4mim][NTf_2]$ with 0.2 M DOHyA/n-DD

$[HNO_3]$/M	Separation factor of Pu(IV) over U(VI)	
	0.02 M DOHyA/ $[C_4mim][NTf_2]$	0.2 M DOHyA/n-DD
0.5	1833	41
1	1000	51
2	360	258
3	152	423
4	100	100
5	78	59

of Pu(IV) was obtained in RTIL diluent ($[C_4mim][NTf_2]$) as compared to that obtained in a molecular diluent, *n*-DD (Figure 2). In addition, the extraction of U(VI) and Am(III) was also carried out in 0.02 M DOHyA/$[C_4mim][NTf_2]$ and compared with the extraction behavior of Pu(IV) at various concentrations of nitric acid. The separation factor of U(VI) over Am(III), Pu(IV) over Am(III) & U(VI) have been compared from distribution ratios and they are tabulated in Table 1. This result indicates that RTILs are creating an option for individual separation of Pu(IV), U(VI) and Am(III) from nitric acid medium using 0.02 M DOHyA in $[C_4mim][NTf_2]$.

Table 2 compares the separation factor of Pu(IV) over U(VI) obtained in 0.02 M DOHyA/ $[C_4mim][NTf_2]$ with that obtained in 0.2 M DOHyA/n-DD. It can be seen that the concentration of DOHyA required in *n*-DD is an order higher than that used in ionic liquid. In spite of this low concentration, the separation factor of Pu(IV) over U(VI) achieved in ionic liquid medium is significantly higher at low nitric acid concentration than that observed in n-DD. Therefore, this study revealed that RTIL diluents offer more advantages than the conventional molecular diluents.

Loading behavior of Europium(III) in RTIL diluent

The third phase formation is an undesirable event in solvent extraction procedures and it is splitting of organic phase into two phases with the heavier one, rich in metal—solvate, and the lighter phase rich in diluent. The heavy phase is known as “Third Phase”. Usually it occurs due to the incompatibility of polar metal-solvate (or acid-solvate) in non-polar hydrocarbon diluents (e.g. n-dodecane) at metal loadings beyond a particular value referred as limiting organic concentration (LOC) and the corresponding aqueous phase

concentration of metal ion is called as critical aqueous concentration (CAC). The formation of third phase creates an inhomogeneous density and changes in the viscosity of organic phase leading to complication in the hydrodynamics of solvent extraction process. The third phase formation is one of the major problems in the extraction of actinides due to the accumulation of fissile elements at third phase, causing criticality concerns. Therefore, elimination of third phase formation is essential for the successful operation of solvent extraction procedures.

Since the ionic liquids are composed entirely of ions, they are strongly polar. Therefore, it is expected that ionic liquids could stabilize the polar metal-solvate complex in organic phase and could prevent the undesirable third phase formation, if ionic liquids are used as diluent in place of conventional diluent, n-dodecane. Hence, it was necessary to understand the loading and third phase formation behavior of metal ion in RTIL. In this context, the loading behavior of Eu(III) in a solution of N,N,N',N'-tetraoctyl diglycolamide (TODGA) present in 1-methyl-3-octylimidazolium bis (trifluoromethanesulfonyl)imide ($[C_8mim][NTf_2]$) ionic liquid medium was studied. In this study, the concentration of Eu(III) was varied from 1 to 95 g/L.

The variation in the loading of Eu(III) in 0.1 M TODGA/$[C_8mim][NTf_2]$ as a function of Eu(III) concentration in 3 M nitric acid phase is shown in Figure 3. It can be seen that the loading of Eu(III) increases marginally with increase in the amount of Eu(III) present in aqueous phase, reaches a plateau at the loading of ~4g/L in ionic liquid phase. This can be attributed to the increased extraction of Eu(III) with increase in the amount of Eu(III) present in aqueous phase followed by saturation in extraction. Since the concentration of nitric acid in nuclear waste could vary from 3 to 4 M, the loading behavior of Eu(III) in 0.1M TODGA/$[C_8mim][NTf_2]$ was also studied at 4 and 5 M HNO_3. The results are also shown in Figure 3. It can be seen that the loading of Eu(III) in ionic liquid phase increases marginally with increase in the concentration of nitric acid in aqueous phase. The Eu(III) loading of ~ 4 to 5 g/L (~0.03 M) was achieved. This observation indicates that Eu(III) could be loaded to the extent of 1:3 (Eu: TODGA) stoichiometry in ionic liquid phase. It is evident from the loading studies that third phase formation was not observed even at the initial concentration of Eu(III) reaches the value of 95 g/L, whereas the third phase formation was reported in 0.1 M TODGA/n-DD at the initial concentration of trivalent metal ion (Nd(III)) reaches the value of ~1.1 g/L in 3 M HNO_3. This study indicates that the ionic liquid, $[C_8mim][NTf_2]$, stabilizes the polar metal solvate (Eu(III)-TODGA) complex in ionic liquid phase and overcomes the undesirable third phase formation.

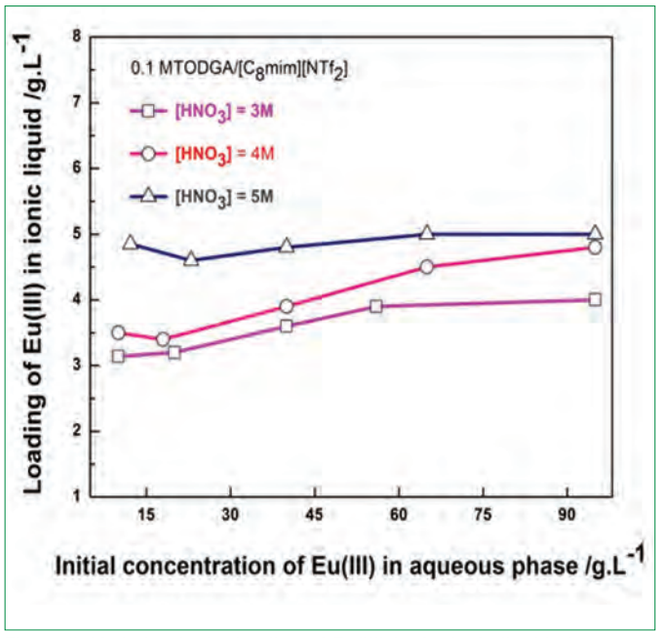

Figure 3: Variation in the loading of Eu(III) in the ionic liquid phase as a function of europium present in aqueous phase

RTIL as extractant

In addition to the role of diluent, RTILs are explored as an extractant. In this aspect, several functionalized ionic liquids (FILs) or task specific ionic liquids (TSILs) in which cationic or anionic part is tethered covalently with organic functionalities have been reported in the recent past. These types of ionic liquids exhibit the properties of both ionic liquid and organic functionality. The use of functionalized ionic liquid could avoid the use of molecular extractants. Since the FILs are usually soluble in ionic liquid diluents, the solvent system is completely devoid of any molecular entities. Therefore, functionalized ionic liquids in nuclear reprocessing applications could offer inherent advantages such as thermal stability and negligible vapor pressure etc. Depending upon the nature of functional group attached, the selectivity of metal ion was found to be different. In this context, a novel phosphoramide functionalized

Table 3: Comparison of separation factor of Pu(IV) over U(VI) obtained in 0.02 M DOHyA/ $[C_4mim][NTf_2]$ with 0.2 M DOHyA/n-DD

$[HNO_3]$/M	Separation factor of actinides in 0.3 M $[BuImPA][NTf_2]/[C_4mim][NTf_2]$		
	$SF_{Pu(IV)/U(VI)}$	$SF_{Pu(IV)/Am(III)}$	$SF_{U(VI)/Am(III)}$
1	3	120	**44**
2	5.5	275	**50**
3	8.3	580	**70**
4	10	1750	**175**
8	15	3500	**240**

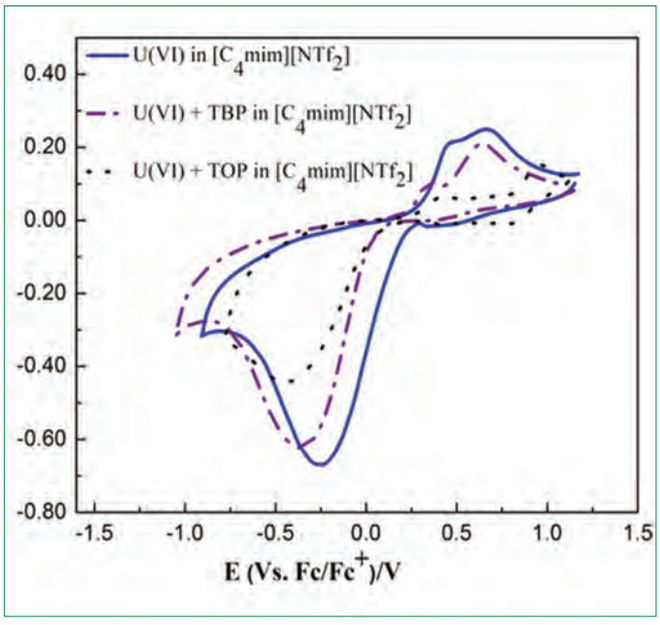

Figure 4: Cyclic voltammogram of U(VI) in $[C_4mim][NTf_2]$, in TBP/$[C_4mim][NTf_2]$ and in TOP/$[C_4mim][NTf_2]$, U(VI) = 0.1 M, [TBP] = [TOP] = 0.03 M, scan rate = 0.1Vs^{-1}, temperature = 373 K.

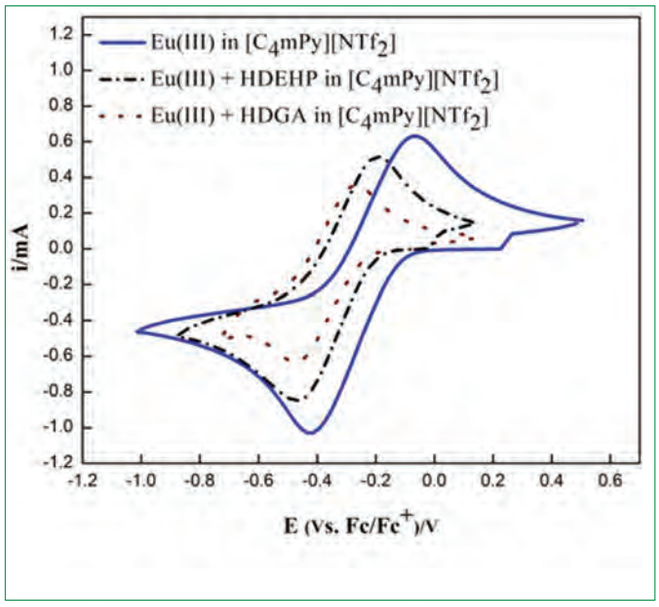

Figure 5: Cyclic voltammogram of Eu(III) in $[C_4mpy][NTf_2]$, in HDGA/$[C_4mpy][NTf_2]$ and in HDEHP/$[C_4mpy][NTf_2]$, [Eu(III)] = 0.1 M, [HDGA]=[HDEHP]= 0.02 M, scan rate = 0.1 Vs^{-1}, temperature = 373 K

ionic liquid, $[BuImPA][NTf_2]$ was synthesized and studied for the extraction of Pu(IV), U(VI) and Am(III) from nitric acid medium.

Extraction of Pu(IV),U(VI) and Am(III) was carried out in 0.3 M $[BuImPA][NTf_2]$ /$[C4mim][NTf_2]$ at various concentrations of nitric acid. The separation factor of U(VI) over Am(III) and Pu(IV) over Am(III) & U(VI) was compared from distribution ratios and they are tabulated in Table 3. This observation indicated the possibility of individual separation of Pu(IV), U(VI) and Am(III) from the mixture of actinides using phosphoramide-FIL.

RTIL as electrolyte medium

In EX-EL approach, RTIL can be used either as extractant or as diluent in conjunction with the molecular extractant, for the liquid-liquid extraction of target metal ions from aqueous feeds. However, unlike the conventional solvent extraction procedure, the extracted metal ion can be recovered by electrodeposition directly from the extracted ionic liquids phase. Therefore, the process holds promise of separating the target metal ion with high separation factor (or decontamination factor), one obtained during liquid-liquid extraction and the other during electrodeposition. Moreover, the metal recovered by electrodeposition is usually in metallic or metal-oxide form such that handling of the final product is easy. In the recent past, there have been increasing studies on the electrochemical behavior of metal ions in the presence of extractants dissolved in RTIL medium. In this direction, electrochemical behavior of U(VI) and Eu(III) was investigated in the presence of molecular extractants dissolved in RTIL electrolytic medium (Figures 4 and 5). The information on metal–ligand stoichiometry and stability constant (lnK_f) of metal-ligand complex was obtained from electrochemical measurements.

The electrochemical behavior of U(VI) in the presence of tri-n-alkyl phosphates (Tri-n-butylphosphate (TBP) and Tri-n-octylphosphate(TOP)) dissolved in $[C_4mim][NTf_2]$ and Eu(III) in the presence of acidic extractants (di(2-ethylhexyl)phosphoric acid (HDEHP) and N,N'-di(2-ethylhexyl) diglycolamic acid (HDGA)) dissolved in $[C_4mpy][NTf_2]$) was investigated. The heterogeneous electron transfer rate constant and the diffusion coefficient of U(VI) and Eu(III) decreased in the order U(VI) > U(VI) – TBP > U(VI) –TOP in $[C_4mim][NTf_2]$ and Eu(III) > (Eu(III) + HDEHP) > (Eu(III) + HDGA) in $[C_4mpy][NTf_2]$. The stability constant (lnK_f) of U(VI)-ligand complex was determined to be 2.7 and 2.9 for U(VI)-TBP and U(VI)-TOP complexes in $[C4mim][NTf_2]$ respectively. Similarly, lnK_f for Eu(III)-HDEHP and Eu(III)- HDGA complexes in $[C_4mpy][NTf_2]$ was found to be 5 and 5.65 respectively.

In summary, RTILs were studied for various applications as diluent and extractant for solvent extraction studies and as electrolytic medium in electrochemical studies of metal ions. The results indicated that RTILs are promising candidates for the nuclear fuel cycle applications.

R. Rama
Materials Chemistry & Metal Fuel Cycle Group

Conference and Meeting Highlights

International Conference on Electron Microscopy and Allied Techniques (EMSI-2017)

July 17 – 19, 2017

Release of Abstract Book and Souvenir during the Inaugural Program

The International Conference on Electron Microscopy and Allied Techniques (EMSI-2017) was organised jointly by IGCAR, IIT Madras and the Electron Microscope Society of India at the Confluence Banquets and Resort during July 17–19, 2017. It was attended by nearly 500 participants from India and abroad which included an inaugural technical address by Dr. S. Banerjee, former Chairman, AEC, two award lectures by Prof. Dipankar Banerjee and GVS Shastry, 28 plenary lectures, 95 invited talks, more than 40 contributory oral presentations in 7 parallel sessions, about 200 posters and 110 photomicrography entries. The conference included a wide range of topics in Materials and Life Sciences. Dedicated sessions included discussions on advances in SEM, TEM and other complimentary and emerging techniques such as Atom Probe Tomography, Fluorescence Microscopy, SPM, STM, Confocal Microscopy, AFM etc. Ten best poster presenters made additional oral presentations and all of them were awarded. The program included a panel discussion on "Micro to Pico Metrology: How far are we from standardization?" Apart of these, there were 4 post conference workshops on Advanced TEM techniques, microtexture, microchemistry and nanomechanical testing in SEM, 3D Atom Probe Tomography and Microscopy in Biological Sciences. The workshops were held at IIT Madras and SRI Guest House, Anupuram during July 20-21, 2017 and were attended by nearly 150 participants.

Arup Dasgupta,Convenor, EMSI-2017

News and Events

Bridge Course on Non-destructive Evaluation (BRIC-NDE)

May 15-19, 2017

Inauguration of Bridge Course on Non-destructive Evaluation (BRIC-NDE) by Dr. Arun Kumar Bhaduri, Director, IGCAR

A Bridge Course on Non-Destructive Evaluation (BRIC-NDE) was organised jointly by IGCAR, QUNEST, SFA Chennai Chapter and ISNT Kalpakkam Chapter at IGCAR during May 15-19, 2017 for the benefit of students completing first year of M. E. / M. Tech (NDT, Metallurgy and Materials/Industrial/Manufacturing/Production/Welding Technology). The objective of this unique course is to motivate the young students by introducing advanced NDE aspects through a series of technical lectures by experts and to provide practical hands-on experience . This course was attended by 45 participants that include 22 motivated students from academic institutes and 23 engineers from IGCAR.

Dr. A.K Bhaduri, Director, IGCAR inaugurated the course on May 15, 2017, after welcome address by Dr. B. P. C Rao, Course Director, BRIC-NDE. During his address, Dr. Bhaduri highlighted the role of NDE in nuclear industry and encouraged the students to learn to the extent possible from this unique course and work for the nation. Dr. G Amarendra, Director, Metallurgy & Materials Group and Materials Science Group, IGCAR highlighted the importance of this course and motivated the students to pursue a research career in NDE.

Expert faculty from NDE and Quality Assurance Divisions of IGCAR and from IIT Madras delivered technical lectures. The lectures were well received and the participants interacted very well with the faculty. During the afternoon sessions, participants performed one mini-project to gain hands-on experience with advanced NDE equipment, apart from lab visits. A quiz competition was conducted on May 18, 2017. During the feedback session on May 19, 2017, the students lauded the bridge course and mentioned that they were immensely benefitted by attending the course. All the students and winners of quiz competition were given certificates.

B. P. C. Rao, Course Director, BRIC-NDE

Participants of Bridge Course on Non-destructive Evaluation (BRIC-NDE) with colleagues of our Centre

News and Events

Summer Training in Physics & Chemistry (STIPAC-2017)

May 29 - July 7, 2017

Participants of Summer Training in Physics & Chemistry (STIPAC-2017) with Prof. V. Aravind, Director, IMSc, Dr. Arun Kumar Bhaduri, Director, IGCAR and senior colleagues of our Centre

IGCAR has been conducting a Summer Training Program in Physics and Chemistry (STIPAC) for the M.Sc. first year students, since 1995. The primary objective of this program is to enthuse and encourage students to take up a career in scientific research. This programme has evolved over the years to train the pre-final post graduate Physics & Chemistry students from across the country both in theoretical & experimental expertise available at IGCAR. Every year, the training course is structured around a theme common to both physics and chemistry.

The theme chosen for this year's programme was "Applications of Electromagnetic Radiation in Physics and Chemistry" and students were asked to send a one page write up on "Electromagnetic Radiation and their use in Scientific Research". Around 200 applications for Physics and 130 applications for Chemistry were received from which 20 students in each discipline were selected, based on their academic credentials, quality of their write-up (Physics) and telephonic interview (Chemistry).

The STIPAC-2017 programme was inaugurated by Prof. V. Aravind, Director, IMSc, Chennai and Dr. A. K. Bhaduri, Director, IGCAR on May 29, 2017. Prof. Aravind gave a special lecture on this occasion on "Computing with Coin Flips: Randomness and Computation".

The program ran for six weeks consisting of about 100 hours of lectures on theory and 50 hours of experiments. In the course of the programme, about 10 special lectures were organized in the evenings by inviting professors from premier institutions. Site visits to MAPS, BHAVINI and UGC-DAE CSR Node facility were also organized.

The valedictory program was held on July 7, 2017 and Prof. V. Chandrasekhar, Director, TIFR-CIS, Hyderabad addressed the students on this day and distributed the certificates. He also gave a special lecture on "Single molecule magnets".

K. Gururaj, K. Prabakar, R. Kumaresan and N. Ramanathan
Coordinators, STIPAC 2017

News and Events

BITS Practice School

May 22 - July 15, 2017

Students from BITS Practice School with Dr. Arun Kumar Bhaduri, Director, IGCAR and senior colleagues of the Centre during valedictory function

Forty nine students from BITS Pilani, Hyderabad and Goa campuses underwent Summer Practice School at our Centre during May 22 - July 15, 2017. This programme is aimed at exposing the students to industrial and research environments, how the organizations work, follow and maintain work ethics, study the core subjects and their applications in the organization, participate in the assignments given to them in the form of projects. Dr. Arun Kumar Bhaduri, Director, IGCAR inaugurated the Practice School programme and interacted with the students. The students were from various disciplines like Computer Science & Engineering, Electrical & Electronics Engineering, Electronics & Instrumentation Engineering, Mechanical Engineering, Economics and Physics. Dr. P. Shankarganesh, BITS Practice School Division, Hyderabad Campus was the programme coordinator. Students carried out challenging projects in various Groups of the Centre according to their discipline. During the period of their stay, they visited various facilities at IGCAR, BHAVINI and MAPS. As a part of the curriculum, quiz, project work presentations, group discussions, report writing and viva were done. Students also participated in Swachh Bharat programme. The valedictory function was held on July 15, 2017 with Dr. Arun Kumar Bhaduri, Director, IGCAR delivering the valedictory address and distributing the certificates to the students.

M. Sai Baba
The then Coordinator-BITS Practice School

News and Events

Graduation Function of the 11th Batch of Trainee Scientific Officers of BARC Training School at IGCAR

July 24, 2017

Release of souvenir at the graduation function Dr. M. Sai Baba, Dr. Sekhar Basu, Dr. Arun Kumar Bhaduri and Dr. Vidya Sundararajan

The 11th batch of thirty three Trainee Scientific Officers from the BARC Training School at IGCAR have successfully completed their training and were graduated in a special ceremony that took place on July 24, 2017. Dr. Sekhar Basu, Chairman, Atomic Energy Commission and Secretary to the Government of India, Department of Atomic Energy was the Chief Guest. Dr. M. Sai Baba, the then Director, Resources Management Group welcomed the gathering. Dr. A. K. Bhaduri, Distinguished Scientist and Director, IGCAR delivered the presidential address. Dr. Sekhar Basu released the souvenir featuring the training school programme during the academic year. Dr. Basu gave away the prestigious 'Homi Bhabha Prizes' comprising of a medallion and books worth Rs. 5000 to the toppers from each discipline and addressed the gathering. He also gave away the course completion certificates to all the graduates passing out. A few of the Trainee Scientific Officers passing out shared their experience, gave a feedback on the academic programme and their stay at the hostel. Dr. Vidya Sundararajan, Head, Strategic Planning and Human Resource Development Division, Resources Management Group, proposed the vote of thanks.

M. Sai Baba, the then Director, RMG

Graduates of BARC Training School at IGCAR with Dr. Sekhar Basu, Chairman, Atomic Energy Commission and Secretary to Government of India, Department of Atomic Energy, Dr. Arun Kumar Bhaduri, Director, IGCAR and senior colleagues of the Centre

News and Events

Quality Circle Annual Meet (QCAM) - 2017

August 30, 2017

Dr. Arun Kumar Bhaduri, Director, IGCAR, delivering the presidential address during the Quality Circle Annual Meet (QCAM) - 2017

Quality circle is a small group of employees doing similar or related work who meet regularly to identify, analyze and solve work related problems usually led by a senior team member. After completing their analysis, they present their solutions to management for implementation and to improve the performance of the organization. Thus, implemented correctly, quality circles can help the organization to reduce costs, increase productivity, and improve employee morale.

In IGCAR, every year Quality Circle Annual Meet (QCAM) is conducted and the QC case studies are presented by the QC teams. QCAM – 2017 was conducted on August 30, 2017 at Convention Centre and SRI Seminar Hall, Anupuram in parallel sessions. Welcome address was delivered by Shri A. Jyothish Kumar, Director, ESG, The Presidential address was delivered by Dr. Arun Kumar Bhaduri, Director, IGCAR. Inaugural Address was delivered by Shri K. Umashankar, Former Senior Manager, BHEL, Chennai and vote of thanks by Shri T V. Maran, EIC, ZWS, FRTG .

Totally 27 Quality Circles from all groups (about 300 members) from IGCAR, Schools from Kalpakkam and neighbourhood presented QC case studies in a wide spectrum of topics covering Technical, Research & Development, Services and Education. Professional judges from QCFI, Chennai adjudged the QC case study presentations. Under the 'Mechanical and Manufacturing' stream, the PLUTONIUM QC Team bagged 'Dr Placid Rodriguez Memorial Trophy', while EXCEL QC team bagged the 'Shri M.K. Ramamurthy memorial trophy' for Plant Operation and Services category.

Prize distribution ceremony during the valedictory function

During valedictory function, the events were summed up by Shri. T. Johny, Head, CWD. The programme concluded with the valedictory address and Shri G. Kempulraj, Former Head, CWD was felicitated for his contribution towards Q.C movement in IGCAR. The prizes were distributed to the participants by Shri A.Jyothish Kumar, Director, ESG and Shri G. Kempulraj, Former Head, CWD. Vote of thanks was proposed by Shri M. Krishnamoorthy, Head, FS, CWD.

T .V. Maran, Member Secretary
Apex Steering Committee on Quality Circles, IGCAR QCAM 2017

Awards and Honours

Dr. Arun Kumar Bhaduri, Distinguished Scientist and Director, IGCAR was conferred with the "Distinguished Alumnus Award" at the 63rd Convocation of Indian Institute of Technology - Kharagpur for his outstanding achievements. He is also the recipient of "Dr. KCG Verghese Excellence Award" for Lifetime Achievement from Hindustan Group of Institutions, Chennai

Dr. S. Ningshen, Corrosion Science and Technology Division, MMG received the "Award for Excellence in Corrosion Science & Technology" for the year 2017, from NACE International Gateway India Section, (NIGIS) during Corrosion Conference and Expo (CORCON-2017) held at Mumbai during September 17-20, 2017

Dr. A. Ravi Shankar, Corrosion Science & Technology Division, MMG received the "Award for Distinction in Corrosion Science & Technology" for the year 2017, from NACE International Gateway India Section, (NIGIS) during Corrosion Conference and Expo (CORCON 2017) held at Mumbai during September 17-20, 2017

Dr. Anish Kumar, Non-Destructive Evaluation Division, MMG has been selected as a "Member of Scientific Advisory Committee to Science & Heritage Research Initiative", Department of Science and Technology (2017-2020)

Shri A. Manivannan, Shri A.V. Vinod, Shri P. Ravisankar, Shri G. Saravanan, Shri S. Maharajan, Smt. R. Jayshree and Shri Madaka Santhosh of Fermi Quality Circle Team of MFFD, MFRG, MC & MFCG had presented their case study and won the awards, "Par Excellance" in the Quality Circle Annual meet 2017 held on August 30, 2017 at SRI Covention Centre, Anupuram and placed in "GOLD "category in the 26th QC Convention of Chennai Chapter" CCQCC-2017 held during September 9-10, 2017 at Sri Sairam Engineering College, Chennai

Best Paper Awards

Synthesis of Fe_3O_4 Magnetic Nanoclusters using Microwave Reactor
Shri. S. Kalyani, Dr. S. Ayyappan and Dr. John Philip
National conference on Nanomaterials (NCN-2017), held at Namakkal during 20-21 July, 2017
Best Paper Award

Anomalous Behaviour of Calcium Chloride Melt Under Cathodic Polarisation Conditions
Ms. Anwesha Mukherjee and Dr. K. S. Mohandas
2nd International Conference on Electrochemical Science and Technology (ICONEST 2017), held at Bengaluru, during 10-12 August, 2017
Best Poster Award

Development of High Temperature Oxidation Resistant SiC interlayer for Ceramic Coating on High Density Graphite
Ms. B. Madhura, Shri. E. Vetrivendan, Dr. Ch. Jagadeeswara Rao, Dr. S. Ningshen and Dr. U. Kamachi Mudali
2nd International Conference on Electrochemical Science and Technology (ICONEST 2017), held at Bengaluru, during 10-12 August, 2017
Best Poster Award

Electrochemical Studies of Zirconium-702 in Concentrated Nitric Acid with and without Fluoride Ions
Dr. J. Jayaraj, Dr. S. Ningshen and Dr. U. Kamachi Mudali
2nd International Conference on Electrochemical Science and Technology (ICONEST 2017), held at Bengaluru, during 10-12 August, 2017
Best Poster Award

Effect of Dead Layer on The Efficiency of Planar Semiconductor Neutron Detectors
Shri Prasanna Gandhiraj, Shri Manoj Kumar Parida, Dr. K. Prabakar, Shri Raghuramaiah Manchi, Dr. S. Tripura Sundari, Dr. J. Jayapandian and Shri Chakram Sampathkumar Sundar
60th Institution of Electronics and Telecommunication Engineers (IETE) Annual Convention, 17 September, 2017
Best Paper Award

Biofilm Analysis on Cooling Waters of Fast Breeder Test Reactor using Advanced Molecular Tools
Dr. B. Anandkumar, Dr. R. P. George, Shri S. Lakshmanapandi, Shri S. Ramamoorthy and Dr. C. Mallika
International Conference on Corrosion-CORCON 2017 held at Mumbai during 17-20 September, 2017
Best Paper Award

Corrosion and Surface Film Characterization of TaNbHfZrTi High Entropy Alloy
Dr. J. Jayaraj, Shri C.Thinaharan, Dr. S. Ningshen, Dr. C. Mallika and Dr. U. Kamachi Mudali
International Conference on Corrosion CORCON-2017 held at Mumbai during 17-20 September, 2017
Best Paper Award

Red wattled Lapwing

Published by Scientific Information Resource Division, RMG, RM&PAG, IGCAR, Kalpakkam-603102